Chapter 6. Electromagnetism

This chapter discusses two major effects that arise when electric and magnetic fields change over time: the "electromagnetic induction" of an additional electric field by changing the magnetic field, and the reciprocal effect of the "displacement currents"– actually, the induction of an additional magnetic field by changing electric field. These two phenomena, which make time-dependent electric and magnetic fields inseparable (hence the term "electromagnetism"[1]), are reflected in the full system of Maxwell equations, valid for an arbitrary electromagnetic process. On the way toward this system, I will make a brief detour to review the electrodynamics of superconductivity, which (besides its own significance), provides a perfect platform for discussion of the important general issue of gauge invariance.

6.1. Electromagnetic induction

As Eqs. (5.36) show, in static situations ($\partial/\partial t = 0$) the Maxwell equations describing the electric and magnetic fields are independent – more exactly, coupled only implicitly, via the continuity equation (4.5) relating their right-hand sides ρ and $\mathbf{j}$. In dynamics, when the fields change in time, the situation is different.

Historically, the first discovered explicit coupling between the electric and magnetic fields was the effect of electromagnetic induction. Although this effect was discovered independently by Joseph Henry, it was a brilliant series of experiments by Michael Faraday, carried out mostly in 1831, that resulted in the first general formulation of the induction law. The summary of Faraday's numerous experiments has turned out to be very simple: if the magnetic flux defined by Eq. (5.65),

$$\Phi \equiv \int_S B_n d^2 r \,, \tag{6.1}$$

through a surface S limited by a closed contour C, changes in time by whatever reason (e.g., either due to a change of the magnetic field $\mathbf{B}$ (as in Fig.1), or the contour's motion, or its deformation, or any combination of the above), it induces an additional, vortex-like electric field $\mathbf{E}_{\text{ind}}$ directed along the contour – see Fig. 1.

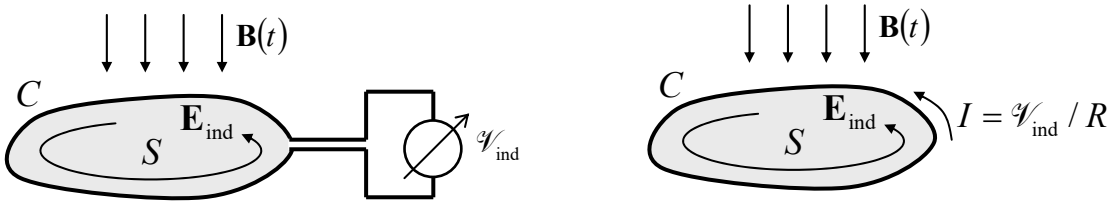

Fig. 6.1. Two simplest ways to observe the Faraday electromagnetic induction.

The exact distribution of $\mathbf{E}_{\text{ind}}$ in space depends on the system's details, but its integral along the contour C, called the *inductive electromotive force* (e.m.f.), obeys a very simple *Faraday induction law*:

[1] It was coined by H. Ørsted in 1820 in the context of his experiments – see the previous chapter.

$$\mathscr{V}_{\rm ind} \equiv \oint_C \mathbf{E}_{\rm ind} \cdot d\mathbf{r} = -\frac{d\Phi}{dt}. \qquad (6.2)$$

Faraday induction law

(In the Gaussian units, the right-hand side of this formula has an additional coefficient of $1/c$.)

It is straightforward (and hence left for the reader's exercise) to show that this e.m.f. may be measured, for example, either by inserting a voltmeter into a conducting loop following the contour C or by measuring the small current $I = \mathscr{V}_{\rm ind}/R$ it induces in a thin wire with a sufficiently large Ohmic resistance R,[2] whose shape follows that contour – see Fig. 1. (Actually, these methods are not entirely different, because a typical voltmeter measures voltage by the small Ohmic current it drives through the pre-calibrated high internal resistance of the device.) In the context of the latter approach, the minus sign in Eq. (2) may be described by the following *Lenz rule*: the magnetic field of the induced current I provides a partial compensation of the *change* of the original flux $\Phi(t)$ with time.[3]

In order to recast Eq. (2) in a differential form, more convenient in many cases, let us apply to the contour integral in it the Stokes theorem, which was repeatedly used in Chapter 5. The result is

$$\mathscr{V}_{\rm ind} = \int_S \left(\nabla \times \mathbf{E}_{\rm ind}\right)_n d^2 r\,. \qquad (6.3)$$

Now combining Eqs. (1)-(3), for a contour C whose shape does not change in time (so that the integration along it is interchangeable with the time derivative), we get

$$\int_S \left(\nabla \times \mathbf{E}_{\rm ind} + \frac{\partial \mathbf{B}}{\partial t}\right)_n d^2 r = 0\,. \qquad (6.4)$$

Since the induced electric field is an addition to the gradient field (1.33) created by electric charges, for the net field we may write $\mathbf{E} = \mathbf{E}_{\rm ind} - \nabla\phi$. However, since the curl of any gradient field is zero,[4] $\nabla\times(\nabla\phi) = 0$, Eq. (4) remains valid even for the net field $\mathbf{E}$. Since this equation should be correct for *any* closed area S, we may conclude that

$$\nabla \times \mathbf{E} + \frac{\partial \mathbf{B}}{\partial t} = 0 \qquad (6.5)$$

Faraday law: differential form

at any point. This is the final (time-dependent) form of this Maxwell equation. Superficially, it may look that Eq. (5) is less general than Eq. (2); for example, it does not describe any electric field, and hence any e.m.f. in a moving loop, if the field $\mathbf{B}$ is constant in time, even if the magnetic flux (1) through the loop does change in time. However, this is not true; in Chapter 9 we will see that in the reference frame moving with the loop, the e.m.f. does appear.[5]

---

[2] Such induced current is sometimes called the *eddy current*, though most often this term is reserved for the distributed currents induced by changing magnetic fields in bulk conductors – see Sec. 3 below.

[3] Let me also hope that the reader is familiar with the paradox arising at attempts to measure $\mathscr{V}_{\rm ind}$ with a voltmeter without its insertion into the wire loop; if not, I would highly recommend them to solve the offered Problem 2.

[4] See, e.g., MA Eq. (11.1).

[5] I have to admit that from the beginning of the course, I was carefully sweeping under the rug a very important question: in what exactly reference frame(s) all the equations of electrodynamics are valid? I promise to discuss this issue in detail later in the course (in Chapter 9), and for now would like to get away with a very short answer: all the formulas discussed so far are valid in *any inertial* reference frame, as defined in classical mechanics – see, e.g., CM Sec. 1.3; however, the fields $\mathbf{E}$ and $\mathbf{B}$ have to be measured *in the same* frame.

Now let us reformulate Eq. (5) in terms of the vector potential **A**. Since the induction effect does not alter the fundamental relation $\nabla \cdot \mathbf{B} = 0$, we still may represent the magnetic field as prescribed by Eq. (5.27), i.e. as $\mathbf{B} = \nabla \times \mathbf{A}$. Plugging this expression into Eq. (5), and changing the order of the temporal and spatial differentiation, we get

$$\nabla \times \left(\mathbf{E} + \frac{\partial \mathbf{A}}{\partial t} \right) = 0 . \tag{6.6}$$

Hence we can use the same argumentation as in Sec. 1.3 (there applied to the vector **E** alone) to represent the expression in the parentheses as $-\nabla\phi$, so we get

Fields via potentials

$$\mathbf{E} = -\frac{\partial \mathbf{A}}{\partial t} - \nabla\phi, \qquad \mathbf{B} = \nabla \times \mathbf{A} . \tag{6.7}$$

It is very tempting to interpret the first term of the right-hand side of the expression for **E** as the one describing the electromagnetic induction alone, and the second term as representing a purely electrostatic field induced by electric charges. However, the separation of these two terms is, to a certain extent, conditional. Indeed, let us consider the gauge transformation already mentioned in Sec. 5.2,

$$\mathbf{A} \to \mathbf{A} + \nabla\chi , \tag{6.8}$$

that, as we already know, does not change the magnetic field. According to Eq. (7), to keep the full electric field intact (*gauge-invariant*) as well, the scalar electric potential has to be transformed simultaneously, as

$$\phi \to \phi - \frac{\partial \chi}{\partial t} , \tag{6.9}$$

leaving the choice of an addition to ϕ restricted only by the Laplace equation – since the full ϕ should satisfy the Poisson equation (1.41) with a gauge-invariant right-hand side. We will return to the discussion of the gauge invariance in Sec. 4.

6.2. Magnetic energy revisited

Now we are sufficiently equipped to revisit the issue of magnetic energy, in particular, to finally prove Eqs. (5.57) and (5.140), and discuss the dichotomy of the signs in Eqs. (5.53) and (5.54). For that, let us consider a sufficiently slow and small magnetic field variation $\delta\mathbf{B}$. If we want to neglect the kinetic energy of the system of electric currents under consideration, as well as the wave radiation effects, we need to prevent its significant acceleration by the arising induction field $\mathbf{E}_{\text{ind}}$. Let us suppose that we do this by virtual balancing of this field by an external electric field $\mathbf{E}_{\text{ext}} = -\mathbf{E}_{\text{ind}}$. According to Eq. (4.38), the work of that field[6] on the stand-alone currents of the system during a small time interval δt, and hence the change of the potential energy of the system, is

$$\delta U = \delta t \int_V \mathbf{j} \cdot \mathbf{E}_{\text{ext}} d^3 r, \qquad \text{so that } \delta U = -\delta t \int_V \mathbf{j} \cdot \mathbf{E}_{\text{ind}} d^3 r , \tag{6.10}$$

[6] As a reminder, the magnetic component of the Lorentz force (5.10), $\mathbf{v}\times\mathbf{B}$, is always perpendicular to the particle velocity **v**, so the magnetic field **B** itself cannot perform any work on moving charges, i.e. on currents.

where the integral is over the volume of the system. Now expressing the current density **j** from the macroscopic Maxwell equation (5.107), $\mathbf{j} = \nabla \times \mathbf{H}$, and then applying the vector algebra identity[7]

$$(\nabla \times \mathbf{H}) \cdot \mathbf{E}_{\text{ind}} \equiv \mathbf{H} \cdot (\nabla \times \mathbf{E}_{\text{ind}}) - \nabla \cdot (\mathbf{E}_{\text{ind}} \times \mathbf{H}), \tag{6.11}$$

we get

$$\delta U = -\delta t \int_V \mathbf{H} \cdot (\nabla \times \mathbf{E}) d^3 r + \delta t \int_V \nabla \cdot (\mathbf{E} \times \mathbf{H}) d^3 r . \tag{6.12}$$

According to the divergence theorem, the second integral in the right-hand of this equality is equal to the flux of the so-called *Poynting vector* $\mathbf{S} \equiv \mathbf{E} \times \mathbf{H}$ through the surface limiting the considered volume *V*. Later in the course we will see that this flux represents, in particular, the power of electromagnetic radiation through the surface. If such radiation is negligible (as it always is if the field variation is sufficiently slow), the surface may be selected sufficiently far, so that the flux of **S** vanishes. In this case, we may express $\nabla \times \mathbf{E}$ from the Faraday induction law (5) to get

$$\delta U = -\delta t \int_V \left(-\frac{\partial B}{\partial t} \right) \cdot \mathbf{H} d^3 r = \int_V \mathbf{H} \cdot \delta \mathbf{B} d^3 r . \tag{6.13}$$

Just as in the electrostatics (see Eqs. (1.65) and (3.73), and their discussion), this relation may be interpreted as the variation of the magnetic field energy *U* of the system, and represented in the form

$$\boxed{\delta U = \int_V \delta u(\mathbf{r}) d^3 r, \qquad \text{with } \delta u \equiv \mathbf{H} \cdot \delta \mathbf{B} .} \tag{6.14}$$

Magnetic energy's variation

This is a keystone result; let us discuss it in some detail.

First of all, for a system filled with a linear and isotropic magnetic material, we may use Eq. (14) together with Eq. (5.110): $\mathbf{B} = \mu \mathbf{H}$. Integrating the result over the variation of the field from 0 to a certain final value **B**, we get Eq. (5.140) – so important that it deserves rewriting again:

$$U = \int_V u(\mathbf{r}) d^3 r, \quad \text{with } u = \frac{B^2}{2\mu} . \tag{6.15}$$

In the simplest case of free space (no magnetics at all, so **j** above is the complete current density), we may take $\mu = \mu_0$, and reduce Eq. (15) to Eq. (5.57). Now performing backward the transformations that took us, in Sec. 5.3, to derive that relation from Eq. (5.54), we finally have the latter formula proved – as was promised in the last chapter.

It is very important, however, to understand the limitations of Eq. (15). For example, let us try to apply it to a very simple problem, which was already analyzed in Sec. 5.6 (see Fig. 5.15): a very long cylindrical sample of a linear magnetic material placed into a fixed external field $\mathbf{H}_{\text{ext}}$ parallel to the sample's length. It is evident that in this simple geometry, the field **H** and hence the field $\mathbf{B} = \mu \mathbf{H}$ have to be uniform inside the sample, besides negligible regions near its ends, so Eq. (15) is reduced to

$$U = \frac{B^2}{2\mu} V , \tag{6.16}$$

[7] See, e.g., MA Eq. (11.7) with $\mathbf{f} = \mathbf{E}_{\text{ind}}$ and $\mathbf{g} = \mathbf{H}$.

where $V = Al$ is the cylinder's volume. Now if we try to calculate the static (equilibrium) value of the field from the minimum of this potential energy, we get evident nonsense: $\mathbf{B} = 0$ (WRONG!).[8]

The situation may be readily rectified by using the notion of the Gibbs potential energy, just as it was done for the electric field in Sec. 3.5 (and implicitly in the end of Sec. 1.3). According to Eq. (14), in magnetostatics, the Cartesian components of the field $\mathbf{H}(\mathbf{r})$ play the role of the generalized forces, while those of the field $\mathbf{B}(\mathbf{r})$, of the generalized coordinates (per unit volume).[9] As the result, the Gibbs potential energy, whose minimum corresponds to the stable equilibrium of the system under the effect of a fixed generalized force (in our current case, of the fixed external field $\mathbf{H}_{\text{ext}}$), is

Gibbs potential energy

$$U_{\text{G}} = \int_V u_{\text{G}}(\mathbf{r})\, d^3 r, \qquad \text{with } u_{\text{G}}(\mathbf{r}) \equiv u(\mathbf{r}) - \mathbf{H}_{\text{ext}}(\mathbf{r}) \cdot \mathbf{B}(\mathbf{r}), \tag{6.17}$$

– the expression parallel to Eq. (3.78). For a system with linear magnetics, we may use, for the energy density $u(\mathbf{r})$, our result (15), getting the following Gibbs energy's density:

$$u_{\text{G}}(\mathbf{r}) = \frac{1}{2\mu}\mathbf{B}\cdot\mathbf{B} - \mathbf{H}_{\text{ext}}\cdot\mathbf{B} \equiv \frac{1}{2\mu}\left(\mathbf{B} - \mu\mathbf{H}_{\text{ext}}\right)^2 + \text{const}, \tag{6.18}$$

where "const" means a term independent of the field $\mathbf{B}$ inside the sample. For our simple cylindrical system, with its uniform fields, Eqs. (17)-(18) gives the following full Gibbs energy of the sample:

$$U_{\text{G}} = \frac{\left(\mathbf{B}_{\text{int}} - \mu\mathbf{H}_{\text{ext}}\right)^2}{2\mu} V + \text{const}, \tag{6.19}$$

whose minimum immediately gives the correct stationary value $\mathbf{B}_{\text{int}} = \mu\mathbf{H}_{\text{ext}}$, i.e. $\mathbf{H}_{\text{int}} \equiv \mathbf{B}_{\text{int}}/\mu = \mathbf{H}_{\text{ext}}$, which was already obtained in Sec. 5.6 in a different way, from the boundary condition (5.117).

Now notice that with this result on hand, Eq. (18) may be rewritten in a different form:

$$u_{\text{G}}(\mathbf{r}) = \frac{1}{2\mu}\mathbf{B}\cdot\mathbf{B} - \frac{\mathbf{B}}{\mu}\cdot\mathbf{B} \equiv -\frac{B^2}{2\mu}, \tag{6.20}$$

similar to Eq. (15) for $u(\mathbf{r})$, but with an opposite sign. This sign dichotomy explains that of Eqs. (5.53) and Eq. (5.54); indeed, as was already noted in Sec. 5.3, the former of these expressions gives the potential energy whose minimum corresponds to the equilibrium of a system with fixed currents. (In our current example, these are the external stand-alone currents inducing the field $\mathbf{H}_{\text{ext}}$.) So, the energy U_j given by Eq. (5.53) is essentially the Gibbs energy U_{G} defined by Eqs. (17) and (for the equilibrium state of linear magnetic media) by Eq. (20), while Eq. (5.54) is just another form of Eq. (15) – as was explicitly shown in Sec. 5.3.[10]

---

[8] This erroneous result cannot be corrected by just adding the energy of the field outside the cylinder because in the limit $A \to 0$, this field is not affected by the internal field $\mathbf{B}$.

[9] Note an aspect in that the analogy with electrostatics is not quite complete. Indeed, according to Eq. (3.76), in electrostatics, the role of a generalized coordinate is played by the "would-be" field $\mathbf{D}$, and that of the generalized force, by the actual (if macroscopic) electric field $\mathbf{E}$. This difference may be traced back to the fact that the electric field $\mathbf{E}$ may perform work on a moving charged particle, while the magnetic field cannot. However, this difference does not affect the full analogy of the expressions (3.73) and (15) for the field energy density in *linear* media.

[10] As was already noted in Sec. 5.4, one more example of the energy U_j (i.e. U_{G}) is given by Eq. (5.100).

Let me complete this section by stating that the difference between the energies U and U_G is not properly emphasized (or even left obscure) in some textbooks, so the reader is advised to get additional clarity by solving a few additional simple problems – for example, by spelling out these energies for a long straight solenoid (Fig. 5.6a), and then using the results to calculate the pressure exerted by the magnetic field on the solenoid's walls (windings) and the longitudinal forces exerted on its ends.

6.3. Quasistatic approximation and skin effect

Perhaps the most surprising experimental fact concerning the time-dependent electromagnetic phenomena is that unless they are so fast that one more new effect of the *displacement currents* (to be discussed in Sec. 7 below) becomes noticeable, all formulas of electrostatics and magnetostatics remain valid, with the only exception: the generalization of Eq. (3.36) to Eq. (5), describing the Faraday induction. As a result, the system of macroscopic Maxwell equations (5.109) is generalized to

$$\nabla\times\mathbf{E}+\frac{\partial\mathbf{B}}{\partial t}=0,\qquad \nabla\times\mathbf{H}=\mathbf{j},$$
$$\nabla\cdot\mathbf{D}=\rho,\qquad \nabla\cdot\mathbf{B}=0. \tag{6.21}$$

Quasistatic approximation

(As it follows from the discussions in chapters 3 and 5, the corresponding system of microscopic Maxwell equations for the genuine, "microscopic" fields **E** and **B** may be obtained from Eq. (21) by the formal substitutions $\mathbf{D}=\varepsilon_0\mathbf{E}$ and $\mathbf{H}=\mathbf{B}/\mu_0$, and the replacement of the stand-alone charge and current densities ρ and **j** with their full densities.[11]) These equations, whose range of validity will be quantified in Sec. 7, define the so-called *quasistatic approximation* of electromagnetism and are sufficient for an adequate description of a broad range of physical effects.

In order to form a complete system of equations, Eqs. (21) should be augmented by constituent equations describing the medium under consideration. For a linear isotropic material, they may be taken in the simplest (and simultaneously, most common) linear and isotropic forms already discussed in Chapters 4 and 5:

$$\mathbf{j}=\sigma\mathbf{E},\qquad \mathbf{B}=\mu\mathbf{H}. \tag{6.22}$$

If the conductor is uniform, i.e. the coefficients σ and μ are constant inside it, the whole system of Eqs. (21)-(22) may be reduced to just one simple equation. Indeed, a sequential substitution of these equations into each other, using a well-known vector-algebra identity[12] in the middle, yields:

$$\frac{\partial\mathbf{B}}{\partial t}=-\nabla\times\mathbf{E}=-\frac{1}{\sigma}\nabla\times\mathbf{j}=-\frac{1}{\sigma}\nabla\times(\nabla\times\mathbf{H})=-\frac{1}{\sigma\mu}\nabla\times(\nabla\times\mathbf{B})\equiv-\frac{1}{\sigma\mu}\left[\nabla(\nabla\cdot\mathbf{B})-\nabla^2\mathbf{B}\right]$$
$$=\frac{1}{\sigma\mu}\nabla^2\mathbf{B}. \tag{6.23}$$

Thus we have arrived, without any further assumptions, at a rather simple partial differential equation. Let us use it for an analysis of the so-called *skin effect*, the phenomenon of an Ohmic conductor's self-shielding from the alternating (*ac*) magnetic field. In its simplest geometry (Fig. 2a), an

[11] Obviously, in free space, the last replacement is unnecessary, because all charges and currents may be treated as "stand-alone" ones.

[12] See, e.g., MA Eq. (11.3).

external source (which, at this point, does not need to be specified) produces, near a plane surface of a bulk conductor, a spatially-uniform ac magnetic field $\mathbf{H}^{(0)}(t)$ parallel to the surface.[13]

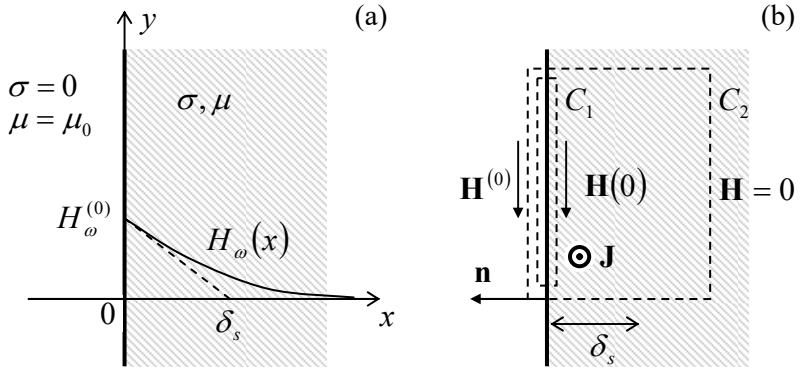

Fig. 6.2. (a) The skin effect in the simplest, planar geometry, and (b) two Ampère contours, C_1 and C_2, for deriving the "macroscopic" (C_1) and the "coarse-grain" (C_2) boundary conditions for **H**.

Selecting the coordinate system as shown in Fig. 2a, we may express this condition as

$$\mathbf{H}\Big|_{x=-0} = H^{(0)}(t)\mathbf{n}_y \,. \tag{6.24}$$

The translational symmetry of our simple problem within the surface plane [y, z] implies that inside the conductor, $\partial/\partial y = \partial/\partial z = 0$ as well, and $\mathbf{H} = H(x, t)\mathbf{n}_y$ even at $x \geq 0$, so Eq. (23) for the conductor's interior is reduced to a differential equation for just one scalar function $H(x, t) = B(x, t)/\mu$:

$$\frac{\partial H}{\partial t} = \frac{1}{\sigma\mu}\frac{\partial^2 H}{\partial x^2}, \qquad \text{for } x \geq 0\,. \tag{6.25}$$

This equation may be further simplified by noticing that due to its linearity, we may use the linear superposition principle for the time dependence of the field,[14] via expanding it, as well as the external field (24), into the Fourier series:

$$\begin{aligned} H(x,t) &= \sum_{\omega} H_{\omega}(x)e^{-i\omega t}, \quad \text{for } x. \geq 0, \\ H^{(0)}(t) &= \sum_{\omega} H_{\omega}^{(0)}e^{-i\omega t}, \qquad \text{for } x = -0, \end{aligned} \tag{6.26}$$

and arguing that if we know the solution for each frequency component of the series, the whole field may be found through the straightforward summation (26) of these solutions.

For each single-frequency component, Eq. (25) is immediately reduced to an ordinary differential equation for the complex amplitude $H_\omega(x)$:[15]

[13] Due to the simple linear relation $\mathbf{B} = \mu\mathbf{H}$ between the fields **B** and **H**, it does not matter too much which of them is used for the solution of this problem, with a slight preference for **H**, due to the simplicity of Eq. (5.117) – the only boundary condition relevant for this simple geometry.

[14] Another way to exploit the linearity of Eq. (6.25) is to use the *spatial-temporal Green's function* approach to explore the dependence of its solutions on various initial conditions. Unfortunately, because of a lack of time, I have to leave an analysis of this opportunity for the reader's exercise.

[15] Let me hope that the reader is not intimidated by the (very convenient) use of such complex variables for describing real fields; their imaginary parts always disappear at the final summation (26). For example, if the

$$-i\omega H_\omega = \frac{1}{\sigma\mu}\frac{d^2}{dx^2}H_\omega . \tag{6.27}$$

From the theory of linear ordinary differential equations, we know that Eq. (27) has the following general solution:

$$H_\omega(x) = H_+ e^{\kappa_+ x} + H_- e^{\kappa_- x}, \tag{6.28}$$

where the constants $\kappa_\pm$ are the roots of the characteristic equation that may be obtained by the substitution of any of these two exponents into the initial differential equation. For our particular case, the characteristic equation following from Eq. (27) is simply

$$-i\omega = \frac{\kappa^2}{\sigma\mu} \tag{6.29}$$

and its roots are, obviously,

$$\kappa_\pm = \left(-i\mu\omega\sigma\right)^{1/2} \equiv \pm\frac{1-i}{\sqrt{2}}\left(\mu\omega\sigma\right)^{1/2}. \tag{6.30}$$

For our problem, the field cannot grow exponentially at $x \to +\infty$, so only one of the coefficients, namely the H_- corresponding to the decaying exponent, with Re $\kappa_- < 0$, may be different from zero, i.e. $H_\omega(x) = H_\omega(0)\exp\{\kappa_- x\}$. To find the constant factor $H_\omega(0)$, we can integrate the macroscopic Maxwell equation $\nabla \times \mathbf{H} = \mathbf{j}$ along a pre-surface contour – say, the contour C_1 shown in Fig. 2b. The right-hand side's integral is negligible because the stand-alone current density $\mathbf{j}$ does not include the "genuinely-surface" currents responsible for the magnetic permeability μ – see Fig. 5.12. As a result, we get the boundary condition similar to Eq. (5.117) for the stationary magnetic field: H_τ = const at $x = 0$, giving us

$$H(0,t) = H^{(0)}(t), \qquad \text{i.e. } H_\omega(0) = H_\omega^{(0)}, \tag{6.31}$$

so the final solution of our boundary problem may be represented as

$$H_\omega(x) = H_\omega^{(0)}\exp\{\kappa_- x\} = H_\omega^{(0)}\exp\left\{-\frac{x}{\delta_s}\right\}\exp\left\{-i\left(\omega t - \frac{x}{\delta_s}\right)\right\}, \tag{6.32}$$

where the constant δ_s, with the dimension of length, is called the *skin depth*:

$$\delta_s \equiv -\frac{1}{\mathrm{Re}\,\kappa_-} = \left(\frac{2}{\mu\sigma\omega}\right)^{1/2}. \tag{6.33}$$

Skin depth

This solution describes the *skin effect*: the penetration of the ac magnetic field, and the eddy currents $\mathbf{j}$, into a conductor only to a finite depth of the order of δ_s. Let me give a few numerical examples of this depth: for copper at room temperature, $\delta_s \approx 1$ cm at the usual ac power distribution frequency of 60 Hz, and is of the order of just 1 μm at a few GHz, i.e. at typical frequencies of cell phone signals and kitchen microwave magnetrons. On the other hand, for lightly salted water, δ_s is close to 250 m at just 1 Hz (with significant implications for radio communications with submarines), and of

external field is purely sinusoidal, with the actual (positive) frequency ω, each sum in Eq. (26) has just two terms, with complex amplitudes H_ω and $H_{-\omega} = H_\omega^*$, so their sum is always real. (For a more detailed discussion of this issue, see, e.g., CM Sec. 5.1.)

the order of 1 cm at a few GHz (explaining, in particular, the nonuniform heating of a soup bowl in a microwave oven).[16]

Let me hope that the equality chain (23) makes the physics of this effect very clear: the external electric field **E**, which is Faraday-induced by an external ac magnetic field, drives the eddy currents **j**, which in turn induce their own magnetic field that eventually (at $x \sim \delta_s$) compensates the external one. Let us quantify these **E** and **j**. Since we have used, in particular, relations $\mathbf{j} = \nabla \times \mathbf{H} = \nabla \times \mathbf{B}/\mu$, and $\mathbf{E} = \mathbf{j}/\sigma$, and spatial differentiation of an exponent yields a similar exponent, the electric field and current density have the same spatial dependence as the magnetic field, i.e. penetrate the conductor only by distances of the order of $\delta_s(\omega)$. Their vectors are directed normally to **B**, while still being parallel to the conductor's surface:[17]

$$\mathbf{j}_\omega(x) = \kappa_- H_\omega(x)\,\mathbf{n}_z, \qquad \mathbf{E}_\omega(x) = \frac{\kappa_-}{\sigma} H_\omega(x)\,\mathbf{n}_z. \tag{6.34}$$

We may use these expressions, in particular, to calculate the time-averaged power density (4.39) of the energy dissipation, for the important case of a sinusoidal ("monochromatic") field $H(x, t) = |H_\omega(x)| \cos(\omega t + \varphi)$, and hence sinusoidal eddy currents: $j(x, t) = |j_\omega(x)| \cos(\omega t + \varphi')$:

$$\bar{\mathcal{P}}(x) = \frac{\overline{j^2(x,t)}}{\sigma} = \frac{|j_\omega(x)|^2 \overline{\cos^2(\omega t + \varphi')}}{\sigma} = \frac{|j_\omega(x)|^2}{2\sigma} = \frac{|\kappa_-|^2 |H_\omega(x)|^2}{2\sigma} = \frac{|H_\omega(x)|^2}{\delta_s^2 \sigma}. \tag{6.35}$$

Now the (elementary) integration of this expression along the *x*-axis (through all the skin depth), using the exponential law (6.32), gives us the following average power of the energy loss per unit area:

Energy loss at skin effect

$$\frac{d\bar{\mathcal{P}}}{dA} \equiv \int_0^\infty \bar{\mathcal{P}}(x)dx = \frac{1}{2\delta_s \sigma}\left|H_\omega^{(0)}\right|^2 \equiv \frac{\mu\omega\delta_s}{4}\left|H_\omega^{(0)}\right|^2. \tag{6.36}$$

We will extensively use this expression in the next chapter to calculate the energy losses in microwave waveguides and resonators with conducting (practically, metallic) walls, and for now let me note only that according to Eqs. (33) and (36), for a fixed magnetic field amplitude, the losses grow with frequency as $\omega^{1/2}$.

One more important remark concerning Eqs. (34): integrating the first of them over *x*, with the help of Eq. (32), we may see that the *linear density* **J** of the surface currents (measured in A/m), is simply and fundamentally related to the applied magnetic field:

$$\mathbf{J}_\omega \equiv \int_0^\infty \mathbf{j}_\omega(x)dx = H_\omega^{(0)}\mathbf{n}_z. \tag{6.37}$$

Since this relation does not have any frequency-dependent factors, we may sum it up for all frequency components, and get a universal relation

$$\mathbf{J}(t) = H^{(0)}(t)\mathbf{n}_z \equiv H^{(0)}(t)(-\mathbf{n}_y \times \mathbf{n}_x) = \mathbf{H}^{(0)}(t) \times (-\mathbf{n}_x) = \mathbf{H}^{(0)}(t) \times \mathbf{n}, \tag{6.38a}$$

[16] Let me hope that the reader's physical intuition makes it evident that the skin effect remains conceptually the same for samples of any *shape*, besides possibly some quantitative details of the field distribution.

[17] The loop (vortex) character of the induced current lines, responsible for the term "eddy", is not very apparent in the 1D geometry explored above, with the near-surface currents (Fig. 2b) looping only implicitly, at $z \to \pm\infty$.

(where $\mathbf{n} = -\mathbf{n}_x$ is the outer normal to the surface – see Fig. 2b) or, in a different form,

$$\Delta\mathbf{H}(t) = \mathbf{n} \times \mathbf{J}(t), \tag{6.38b}$$

Coarse-grain boundary relation

where $\Delta\mathbf{H}$ is the full change of the field through the skin layer. This simple *coarse-grain relation* (independent of the choice of coordinate axes), is also independent of the used constituent relations (22), and is by no means occasional. Indeed, it may be readily obtained from the macroscopic Ampère law (5.116), by applying it to a contour drawn around a fragment of the surface, extending under it substantially deeper than the skin depth – see the contour C_2 in Fig. 2b. Hence, Eq. (38) is valid regardless of the exact law of the field penetration.

For the skin effect, this fundamental relationship between the linear current density and the external magnetic field implies that the skin effect's implementation does not necessarily require a dedicated ac magnetic field source. For example, the effect takes place in any wire that carries an ac current, leading to a current's concentration in a surface sheet of thickness $\sim\delta_s$. (Of course, the quantitative analysis of this problem in a wire with an arbitrary cross-section may be technically complicated, because it requires solving Eq. (23) for the corresponding 2D geometry; even for the round cross-section, the solution involves the Bessel functions.) In this case, the ac magnetic field outside the conductor, which still obeys Eq. (38), may be better interpreted as the effect, rather than the cause, of the ac current flow.

Finally, please mind the limited validity of all the above results. First, for the quasistatic approximation to be valid, the field frequency ω should not be too high, so the displacement current effects are negligible. (Again, this condition will be quantified in Sec. 7 below; it will show that for metals, the condition is violated only at extremely high frequencies above $\sim 10^{18}$ s^{-1}.) A more practical upper limit on ω is that the skin depth δ_s should stay much larger than the mean free path l of charge carriers,[18] because beyond this point, the constituent relation between the vectors $\mathbf{j}(\mathbf{r})$ and $\mathbf{E}(\mathbf{r})$ becomes essentially *non-local*. Both theory and experiment show that at δ_s below l, the skin effect persists, but acquires a frequency dependence slightly different from Eq. (33): $\delta_s \propto \omega^{-1/3}$ rather than $\omega^{-1/2}$. Historically, this *anomalous skin effect* has been very useful for the measurements of the Fermi surfaces of metals.[19]

6.4. Electrodynamics of superconductivity, and the gauge invariance

The effect of superconductivity[20] takes place (in certain materials only, mostly metals) when temperature T is reduced below a certain *critical temperature* T_c specific for each material. For most metallic superconductors, T_c is of the order of typically a few kelvins, though several compounds (the so-called *high-temperature superconductors*) with T_c above 100 K have been found since 1987. The most notable property of superconductors is the absence, at $T < T_c$, of measurable resistance to (not very high) dc currents. However, the electromagnetic properties of superconductors cannot be described by just taking $\sigma = \infty$ in our previous results. Indeed, for this case, Eq. (33) would give $\delta_s = 0$, i.e., no ac

[18] A discussion of the mean free path may be found, for example, in SM Chapter 6. In very clean metals at very low temperatures, δ_s may approach l at frequencies as low as ~1 GHz, but at room temperature, the crossover between the normal to the anomalous skin effect takes place only at ~ 100 GHz.

[19] See, e.g., A. Abrikosov, *Introduction to the Theory of Normal Metals*, Academic Press, 1972.

[20] Discovered experimentally in 1911 by Heike Kamerlingh Onnes.

magnetic field penetration at all. Experiment shows something substantially different: weak magnetic fields do penetrate into superconductors by a material-specific distance $\delta_L \sim 10^{-7}$-10^{-6} m, the so-called *London's penetration depth*,[21] which is virtually frequency-independent until the skin depth δ_s, of the same material in its "normal" state, i.e. the absence of superconductivity, becomes less than δ_L. (This crossover happens typically at frequencies $\omega \sim 10^{13}$-10^{14} s^{-1}.) The smallness of δ_L on the human scale means that the magnetic field is pushed out from macroscopic samples at their transition into the superconducting state.

This *Meissner-Ochsenfeld effect*, discovered experimentally in 1933,[22] may be partly understood using the following classical reasoning. Our discussion of the Ohm law in Sec. 4.2 implied that the current's (and hence the electric field's) frequency ω is either zero or sufficiently low. In the classical Drude reasoning, this is acceptable while $\omega\tau << 1$, where τ is the effective carrier scattering time participating in Eqs. (4.12)-(4.13). If this condition is not satisfied, we should take into account the charge carrier inertia; moreover, in the opposite limit $\omega\tau >> 1$, we may neglect the scattering at all. Classically, we can describe the charge carriers in such a "perfect conductor" as particles with a non-zero mass m, which are accelerated by the electric field following the 2nd Newton law (4.11),

$$m\dot{\mathbf{v}} = \mathbf{F} = q\mathbf{E}, \tag{6.39}$$

so the current density $\mathbf{j} = qn\mathbf{v}$ that they create, changes in time as

$$\dot{\mathbf{j}} = qn\dot{\mathbf{v}} = \frac{q^2 n}{m}\mathbf{E}. \tag{6.40}$$

In terms of the Fourier amplitudes of the functions $\mathbf{j}(t)$ and $\mathbf{E}(t)$, this means

$$-i\omega \mathbf{j}_\omega = \frac{q^2 n}{m}\mathbf{E}_\omega. \tag{6.41}$$

Comparing this formula with the relation $\mathbf{j}_\omega = \sigma\mathbf{E}_\omega$ implied in the last section, we see that we can use all its results with the following replacement:

$$\sigma \to i\frac{q^2 n}{m\omega}. \tag{6.42}$$

This change replaces the characteristic equation (29) with

$$-i\omega = \frac{\kappa^2 m\omega}{iq^2 n\mu}, \qquad \text{i.e. } \kappa^2 = \frac{\mu q^2 n}{m}, \tag{6.43}$$

i.e. replaces the skin effect with the field penetration by the following frequency-independent depth:

$$\delta \equiv \frac{1}{\kappa} = \left(\frac{m}{\mu q^2 n}\right)^{1/2}. \tag{6.44}$$

Superficially, this means that the field decay into the superconductor does not depend on frequency:

[21] Named so to acknowledge the pioneering theoretical work of brothers Fritz and Heinz London – see below.

[22] It is hardly fair to shorten this name to just the "Meissner effect" as it is frequently done, because of the reportedly crucial contribution by Robert Ochsenfeld, then a Walther Meissner's student, to the discovery.

$$H(x,t) = H(0,t)e^{-x/\delta}, \tag{6.45}$$

thus explaining the Meissner-Ochsenfeld effect.

However, there are two problems with this result. First, for the parameters typical for good metals ($q = -e$, $n \sim 10^{29}$ m^{-3}, $m \sim m_e$, $\mu \approx \mu_0$), Eq. (44) gives $\delta \sim 10^{-8}$ m, one or two orders of magnitude lower than the experimental values of δ_L. Experiment also shows that the penetration depth diverges at $T \to T_c$, which is not predicted by Eq. (44).

The second, much more fundamental problem with Eq. (44) is that it has been derived for $\omega\tau >> 1$. Even if we assume that somehow there is no scattering at all, i.e. $\tau = \infty$, at $\omega \to 0$ both parts of the characteristic equation (43) vanish, and we cannot make any conclusion about κ. This is not just a mathematical artifact we could ignore. For example, let us place a non-magnetic metal into a static external magnetic field at $T > T_c$. The field would completely penetrate the sample. Now let us cool it. As soon as the temperature is decreased below T_c, the above calculations would become valid, forbidding the penetration into the superconductor of any *change* of the field, so the initial field would be "frozen" inside the sample. The Meissner-Ochsenfeld experiments have shown something completely different: as T is lowered below T_c, the initial field is being expelled out of the sample.

The resolution of these contradictions is provided by quantum mechanics. As was explained in 1957 in a seminal work by J. Bardeen, L. Cooper, and J. Schrieffer (commonly referred to as the *BCS theory*), superconductivity is due to the correlated motion of electron pairs, with opposite spins and nearly opposite momenta. Such *Cooper pairs*, each with the electric charge $q = -2e$ and zero spin, may form only in a narrow energy layer near the Fermi surface, of a certain thickness $\Delta(T)$. This parameter $\Delta(T)$, which may be also interpreted as the binding energy of the pair, tends to zero at $T \to T_c$, while at $T << T_c$ it has a virtually constant value $\Delta(0) \approx 3.5\, k_B T_c$, of the order of a few meV for most superconductors. This fact readily explains the relatively low spatial density of the Cooper pairs: $n_p \sim n\Delta(T)/\varepsilon_F \sim 10^{26}$ m^{-3}. With the correction $n \to n_p$, Eq. (44) for the penetration depth becomes

$$\delta \to \delta_L = \left(\frac{m}{\mu q^2 n_p}\right)^{1/2}. \tag{6.46}$$

London's penetration depth

This result diverges at $T \to T_c$, and generally fits the experimental data reasonably well, at least for the so-called "clean" superconductors with the mean free path $l = v_F\tau$ (where $v_F \sim (2m\varepsilon_F)^{1/2}$ is the r.m.s. velocity of electrons on the Fermi surface) much longer than the Cooper pair size ξ – see below.

The smallness of the coupling energy $\Delta(T)$ is also a key factor in the explanation of the Meissner-Ochsenfeld effect. Because of Heisenberg's quantum uncertainty relation $\delta r \delta p \sim \hbar$, the spatial extension of the Cooper-pair's wavefunction (the so-called *coherence length* of the superconductor) is relatively large: $\xi \sim \delta r \sim \hbar/\delta p \sim \hbar v_F/\Delta(T) \sim 10^{-6}$ m. As a result, $n_p\xi^3 >> 1$, meaning that the wavefunctions of the pairs are strongly overlapped in space. Due to their integer spin, Cooper pairs behave like bosons, which means in particular that at low temperatures they exhibit the so-called *Bose-Einstein condensation* onto the same ground energy level ε_g.[23] This means that the quantum frequency ω

[23] A quantitative discussion of the Bose-Einstein condensation of bosons may be found in SM Sec. 3.4, though the full theory of superconductivity is more complicated because it has to describe the condensation taking place *simultaneously* with the formation of effective bosons (Cooper pairs) from fermions (single electrons). For a

$= \varepsilon_g/\hbar$ of the time evolution of each pair's wavefunction $\Psi = \psi\exp\{-i\omega t\}$ is exactly the same and that the phases φ of the wavefunctions, defined by the relation

$$\psi = |\psi| e^{i\varphi}, \tag{6.47}$$

coincide, so the electric current is carried not by individual Cooper pairs but rather by their *Bose-Einstein condensate* described by a single wavefunction (47). Due to this coherence, the quantum effects (which are, in the usual Fermi-gases of single electrons, masked by the statistical spread of their energies, and hence of their phases), become very explicit – "macroscopic".

To illustrate this, let us write the well-known quantum-mechanical formula for the probability current density of a free, non-relativistic particle,[24]

$$\mathbf{j}_w = \frac{i\hbar}{2m}\left(\psi\nabla\psi^* - \text{c.c.}\right) \equiv \frac{1}{2m}\left[\psi^*\left(-i\hbar\nabla\right)\psi - \text{c.c.}\right], \tag{6.48}$$

where c.c. means the complex conjugate of the previous expression. Now let me borrow one result that will be proved later in this course (in Sec. 9.7) when we discuss the analytical mechanics of a charged particle moving in an electromagnetic field. Namely, to account for the magnetic field effects, the particle's *kinetic momentum* $\mathbf{p} \equiv m\mathbf{v}$ (where $\mathbf{v} \equiv d\mathbf{r}/dt$ is the particle's velocity) has to be distinguished from its *canonical momentum*,[25]

$$\mathbf{P} \equiv \mathbf{p} + q\mathbf{A}. \tag{6.49}$$

where $\mathbf{A}$ is the field's vector potential defined by Eq. (5.27). In contrast with the Cartesian components $p_j = mv_j$ of the kinetic momentum $\mathbf{p}$, the canonical momentum's components are the generalized momenta corresponding to the Cartesian components r_j of the radius-vector $\mathbf{r}$, considered as generalized coordinates of the particle: $P_j = \partial\mathscr{L}/\partial v_j$, where $\mathscr{L}$ is the particle's Lagrangian function. According to the general rules of transfer from classical to quantum mechanics,[26] it is the vector $\mathbf{P}$ whose operator (in the coordinate representation) equals $-i\hbar\nabla$, so the operator of the kinetic momentum $\mathbf{p} = \mathbf{P} - q\mathbf{A}$ is $-i\hbar\nabla + q\mathbf{A}$. Hence, to account for the magnetic field[27] effects, we should make the following replacement,

$$-i\hbar\nabla \to -i\hbar\nabla - q\mathbf{A}, \tag{6.50}$$

in all quantum-mechanical relations. In particular, Eq. (48) has to be generalized as

$$\mathbf{j}_w = \frac{1}{2m}\left[\psi^*\left(-i\hbar\nabla - q\mathbf{A}\right)\psi - \text{c.c.}\right]. \tag{6.51}$$

This expression becomes more transparent if we take the wavefunction in form (47); then

---

detailed, but still very readable coverage of the physics of superconductors, I can recommend the reader the monograph by M. Tinkham, *Introduction to Superconductivity*, 2nd ed., McGraw-Hill, 1996.

[24] See, e.g., QM Sec. 1.4, in particular Eq. (1.47).

[25] I am sorry to use traditional notations $\mathbf{p}$ and $\mathbf{P}$ for the momenta – the same symbols which were used for the electric dipole moment and polarization in Chapter 3. I hope there will be no confusion because the latter notions are not used in this section.

[26] See, e.g., CM Sec. 10.1, in particular Eq. (10.26).

[27] The account of the electric field is easier, because the related energy $q\phi$ of the particle may be directly included in the potential energy operator.

$$\mathbf{j}_w = \frac{\hbar}{m}|\psi|^2\left(\nabla\varphi - \frac{q}{\hbar}\mathbf{A}\right). \tag{6.52}$$

This relation means, in particular, that in order to keep $\mathbf{j}_w$ gauge-invariant, the transformation (8)-(9) has to be accompanied by a simultaneous transformation of the wavefunction's phase:

$$\varphi \to \varphi + \frac{q}{\hbar}\chi\,. \tag{6.53}$$

It is fascinating that the quantum-mechanical wavefunction (or more exactly, its phase) is *not* gauge-invariant, meaning that you may change it in your mind – at your free will! Again, this does not change any observable (such as $\mathbf{j}_w$ or the probability density $\psi\psi^*$), i.e. any experimental results.

Now for the *electric* current density of the whole superconducting condensate, Eq. (52) yields the following constitutive relation:

$$\mathbf{j} \equiv \mathbf{j}_w q n_{\rm p} = \frac{\hbar q n_{\rm p}}{m}|\psi|^2\left(\nabla\varphi - \frac{q}{\hbar}\mathbf{A}\right), \tag{6.54}$$

Supercurrent density

The formula shows that this *supercurrent* may be induced by the dc magnetic field alone and does not require any electric field. Indeed, for the simple 1D geometry shown in Fig. 2a, $\mathbf{j}(\mathbf{r}) = j(x)\mathbf{n}_z$, $\mathbf{A}(\mathbf{r}) = A(x)\mathbf{n}_z$, and $\partial/\partial z = 0$, so the Coulomb gauge condition (5.48) is satisfied for any choice of the gauge function $\chi(x)$. For the sake of simplicity we can choose this function to provide $\varphi(\mathbf{r}) \equiv$ const,[28] so

$$\mathbf{j} = -\frac{q^2 n_{\rm p}}{m}\mathbf{A} \equiv -\frac{1}{\mu\delta_{\rm L}^2}\mathbf{A}\,. \tag{6.55}$$

where $\delta_{\rm L}$ is given by Eq. (46), and the field is assumed to be small and hence not affecting the probability $|\psi|^2$ (here normalized to 1 in the absence of the field). This is the so-called *London equation*, proposed (in a different form) by F. and H. London in 1935 for the Meissner-Ochsenfeld effect's explanation. Combining it with Eq. (5.44), generalized for a linear magnetic medium by the replacement $\mu_0 \to \mu$, we get

$$\nabla^2\mathbf{A} = \frac{1}{\delta_{\rm L}^2}\mathbf{A}\,, \tag{6.56}$$

For our 1D geometry, this simple differential equation, similar to Eq. (23), has an exponential solution similar to Eq. (32):

$$A(x) = A(0)\exp\left\{-\frac{x}{\delta_{\rm L}}\right\}, \qquad B(x) = B(0)\exp\left\{-\frac{x}{\delta_{\rm L}}\right\}, \qquad j(x) = j(0)\exp\left\{-\frac{x}{\delta_{\rm L}}\right\}, \tag{6.57}$$

which shows that the magnetic field and the supercurrent penetrate into a superconductor only by London's penetration depth $\delta_{\rm L}$, regardless of frequency.[29] By the way, integrating the last result through the penetration layer, and using the vector potential's definition, $\mathbf{B} = \nabla\times\mathbf{A}$ (for our geometry, giving

[28] This is the so-called *London gauge*; for our simple geometry, it is also the Coulomb gauge (5.48).

[29] Since at $T > 0$, not all electrons in a superconductor form Cooper pairs, at any frequency $\omega \neq 0$ the unpaired electrons provide energy-dissipating Ohmic currents, which are not described by Eq. (54). These losses become very substantial when the frequency ω becomes so high that the skin-effect length $\delta_{\rm s}$ of the material becomes less than $\delta_{\rm L}$. For typical metallic superconductors, this crossover takes place at frequencies of a few hundred GHz, so even for microwaves, Eq. (57) still gives a fairly accurate description of the field penetration.

$B(x) = dA(x)/dx = -\delta_L A(x)$) we may readily verify that the linear density **J** of the surface supercurrent still satisfies the universal coarse-grain relation (38).

This universality should bring to our attention the following common feature of the skin effect (in "normal" conductors) and the Meissner-Ochsenfeld effect (in superconductors): if the linear size of a bulk sample is much larger than, respectively, δ_s or δ_L, than **B** = 0 in the dominating part of its interior. According to Eq. (5.110), a formal description of such conductors (valid only on a coarse-grain scale much larger than either δ_s or δ_L), may be achieved by formally treating the sample as an *ideal diamagnet*, with $\mu = 0$. In particular, we can use this description and Eq. (5.124) to immediately obtain the magnetic field's distribution outside of a bulk sphere:

$$\mathbf{B} = \mu_0 \mathbf{H} = -\mu_0 \nabla \phi_m, \qquad \text{with } \phi_m = H_0 \left(-r - \frac{R^3}{2r^2} \right) \cos\theta, \qquad \text{for } r \geq R. \tag{6.58}$$

Figure 3 shows the corresponding surfaces of equal potential ϕ_m. It is evident that the magnetic field lines (which are normal to the equipotential surfaces) bend to become parallel to the surface near it.

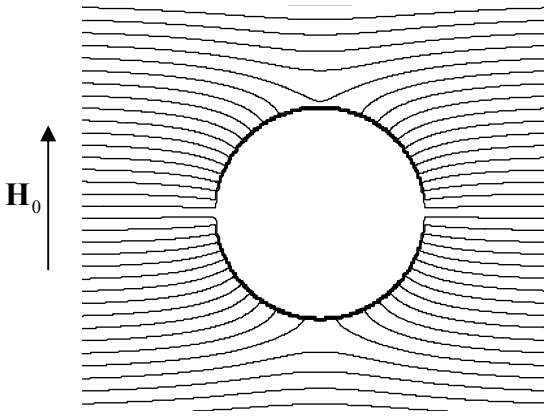

Fig. 6.3. Equipotential surfaces ϕ_m = const around a conducting sphere of radius $R >> \delta_s$ (or δ_L), placed into a uniform magnetic field, calculated within the coarse-grain (ideal-diamagnet) approximation $\mu = 0$.

This pattern also helps to answer the question that might arise at making the assumption (24): what happens to bulk conductors placed into a *normal* ac magnetic field – and to superconductors in a normal dc magnetic field as well? The answer is: the field is deformed outside of the conductor to sustain the following *coarse-grain boundary condition*:[30]

Coarse-grain boundary condition

$$B_n\big|_{\text{surface}} = 0, \tag{6.59}$$

which follows from Eq. (5.118) and the coarse-grain requirement $\mathbf{B}|_{\text{inside}} = 0$.

This answer should be taken with reservations. For normal conductors, it is only valid at sufficiently high frequencies where the skin depth (33) is relatively small: $\delta_s << a$, where a is the scale of the conductor's linear size – for a sphere, $a \sim R$. In superconductors, this simple picture requires not only that $\delta_s << a$, but also that magnetic field is relatively low because strong fields *do* penetrate

[30] Sometimes this boundary condition, as well as the (compatible) Eq. (38), are called "macroscopic". However, this term may lead to confusion with the genuine macroscopic boundary conditions (5.117)-(5.118), which also ignore the atomic-scale microstructure of the "effective currents" $\mathbf{j}_{ef} = \nabla \times \mathbf{M}$, but (as was shown earlier in this section) still allow explicit, detailed accounts of the skin-current (34) and supercurrent (55) distributions.

superconductors, destroying superconductivity (either completely or partly), and as a result violating the Meissner-Ochsenfeld effect – see the next section.

6.5. Electrodynamics of macroscopic quantum phenomena[31]

Despite the superficial similarity of the skin effect and the Meissner-Ochsenfeld effect, the electrodynamics of superconductors is much richer. For example, let us use Eq. (54) to describe the fascinating effect of *magnetic flux quantization*. Consider a closed ring/loop (not necessarily a round one) made of a superconducting "wire" with a cross-section much larger than δ_L^2 (Fig. 4a).

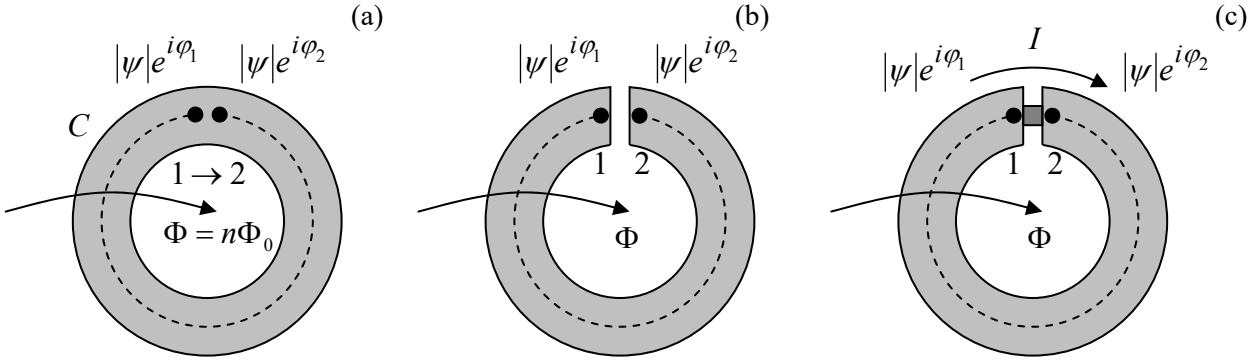

Fig. 6.4. (a) A closed, flux-quantizing superconducting ring, (b) a ring with a narrow slit, and (c) a Superconducting QUantum Interference Device (SQUID).

From the last section's discussion, we know that deep inside the wire the supercurrent is exponentially small. Integrating Eq. (54) along any closed contour C that does not approach the surface closer than a few δ_L at any point (see the dashed line in Fig. 4), so with $\mathbf{j} = 0$ at all its points, we get

$$\oint_C \nabla\varphi \cdot d\mathbf{r} - \frac{q}{\hbar}\oint_C \mathbf{A} \cdot d\mathbf{r} = 0 . \tag{6.60}$$

The first integral, i.e. the difference of φ in the initial and final points, has to be equal to either zero or an integer number of 2π because the change $\varphi \to \varphi + 2\pi n$ does not change the Cooper pair's condensate's wavefunction:

$$\psi' \equiv |\psi| e^{i(\varphi + 2\pi n)} = |\psi| e^{i\varphi} \equiv \psi . \tag{6.61}$$

On the other hand, according to Eq. (5.65), the second integral in Eq. (60) is just the magnetic flux Φ through the contour.[32] As a result, we get a wonderful result:

[31] The material of this section is not covered in most E&M textbooks, and will not be used in later sections of this course. Thus the "only" loss due to the reader's skipping this section would be the lack of familiarity with one of the most fascinating fields of physics. Note also that we already have virtually all formal tools necessary for its discussion, so reading this section should not require much effort.

[32] Due to the Meissner-Ochsenfeld effect, the exact path of the contour is not important, and we may discuss Φ just as the magnetic flux through the ring.

Magnetic flux quantization

$$\Phi = n\Phi_0, \quad \text{where } \Phi_0 \equiv \frac{2\pi\hbar}{|q|}, \quad \text{with } n = 0, \pm 1, \pm 2, \ldots, \tag{6.62}$$

saying that the magnetic flux inside any superconducting loop can only take values multiple of the *flux quantum* Φ_0. This effect, predicted in 1950 by the same Fritz London (who expected q to be equal to the electron charge $-e$), was observed experimentally in 1961,[33] but with $|q| = 2e$ – so $\Phi_0 \approx 2.07\times10^{-15}$ Wb. Historically, this observation gave decisive support to the BCS theory of superconductivity (implying Cooper pairs with charge $q = -2e$) that had been put forward just four years earlier.

Note the truly macroscopic character of this quantum effect: it has been repeatedly observed in human-scale superconducting loops, and from what is known about superconductors, there is no doubt that if we had made a giant superconducting wire loop extending, say, over the Earth's equator, the magnetic flux through it would still be quantized – though with a very large flux quanta number n. This means that the quantum coherence of Bose-Einstein condensates may extend over, using H. Casimir's famous expression, "miles of dirty lead wire". (Lead is a typical superconductor, with $T_c \approx 7.2$ K, and indeed retains its superconductivity even being highly contaminated by impurities.)

Moreover, hollow rings are not entirely necessary for flux quantization. In 1957, A. Abrikosov explained the counter-intuitive high-field behavior of superconductors with $\delta_L > \xi\sqrt{2}$, known experimentally as their *mixed* (or "Shubnikov") *phase* since the 1930s. He showed that a sufficiently high magnetic field may penetrate such superconductors in the form of self-formed magnetic field "threads" (or "tubes") surrounded by vortex-shaped supercurrents – the so-called *Abrikosov vortices.* In the simplest case, the core of such a vortex is a straight line, on which the superconductivity is completely suppressed ($|\psi| = 0$), surrounded by circular, axially-symmetric, persistent supercurrents $\mathbf{j}(\rho)$, where ρ is the distance from the vortex axis – see Fig. 5a. At the axis, the current vanishes, and with the growth of ρ, it first rises and then falls (with $\mathbf{j}(\infty) = 0$), reaching its maximum at $\rho \sim \xi$, while the magnetic field $\mathbf{B}(\rho)$, directed along the vortex axis, is largest at $\rho = 0$, and drops monotonically at distances of the order of δ_L (Fig. 5b).

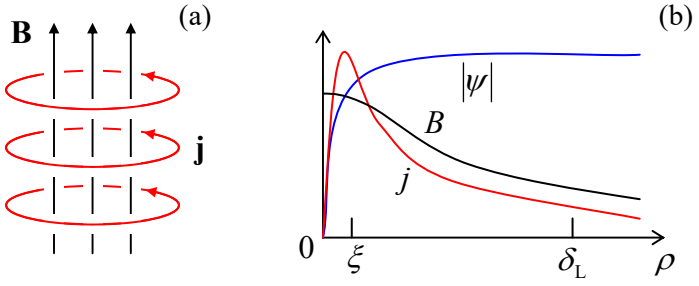

Fig. 6.5. The Abrikosov vortex: (a) a 3D structure's sketch, and (b) the main variables as functions of the distance ρ from the axis (schematically).

The total flux of the field equals exactly one flux quantum Φ_0, given by Eq. (62). Correspondingly, the wavefunction's phase φ performs just one $\pm2\pi$ revolution along *any* contour drawn around the vortex's axis, so $\nabla\varphi = \pm\mathbf{n}_\varphi/\rho$, where $\mathbf{n}_\varphi$ is the azimuthal unit vector.[34] This topological feature of the wavefunction's phase is sometimes called *fluxoid quantization* – to distinguish it from

[33] Independently and virtually simultaneously by two groups: B. Deaver and W. Fairbank, and R. Doll and M. Näbauer; their reports were published back-to-back in the same issue of the *Physical Review Letters*.

[34] The last (perhaps, evident) expression for $\nabla\varphi$ follows from MA Eq. (10.2) with $f = \pm\varphi + \text{const}$.

magnetic *flux quantization*, which is valid only for relatively large contours, not approaching the axis by distances $\sim\delta_L$.

A quantitative analysis of Abrikosov vortices requires, besides the equations we have discussed, one more constituent relation that would describe the suppression of the number of Cooper pairs (quantified by $|\psi|^2$) by the magnetic field – or rather by the field-induced supercurrent. In his original work, Abrikosov used for this purpose the famous *Ginzburg-Landau* equation,[35] which is quantitatively valid only at $T \approx T_c$. The equation may be conveniently represented in either of the following two forms:

$$\frac{1}{2m}\left(-i\hbar\nabla - q\mathbf{A}\right)^2\psi = a\psi - b\psi|\psi|^2, \qquad \xi^2\psi^*\left(\nabla - i\frac{q}{\hbar}\mathbf{A}\right)^2\psi = \left(1-|\psi|^2\right)|\psi|^2, \tag{6.63}$$

where a and b are certain temperature-dependent coefficients, with $a \to 0$ at $T \to T_c$. The first of these forms clearly shows that the Ginzburg-Landau equation (as well as the similar *Gross-Pitaevskii* equation describing electrically-neutral Bose-Einstein condensates) belongs to a broader class of *nonlinear Schrödinger equations*, differing from the usual Schrödinger equation, which is linear in ψ, only by the additional nonlinear terms. The equivalent, second form of Eq. (63) is more convenient for applications and shows more clearly that if the superconductor's condensate density, proportional to $|\psi|^2$, is suppressed only locally, it self-restores to its unperturbed value (with $|\psi|^2 = 1$) at the distances of the order of the coherence length $\xi \equiv \hbar/(2ma)^{1/2}$.

This fact enables a simple quantitative analysis of the Abrikosov vortex in the most important limit $\xi << \delta_L$. Indeed, as Fig. 5 shows, in this case. $|\psi|^2 = 1$ at most distances ($\rho \sim \delta_L$) where the field and current are distributed, so these distributions may be readily calculated without any further involvement of Eq. (63), just from Eq. (54) with $\nabla\varphi = \pm\mathbf{n}_\varphi/\rho$, and the Maxwell equations (21) for the magnetic field, giving $\nabla\times\mathbf{B} = \mu\mathbf{j}$, and $\nabla\cdot\mathbf{B} = 0$. Indeed, combining these equations just as this was done at the derivation of Eq. (23), for the only Cartesian component of the vector $\mathbf{B}(\mathbf{r}) = B(\rho)\mathbf{n}_z$ (where the z-axis is directed along the vortex' symmetry axis), we get a simple equation

$$\delta_L^2\nabla^2 B - B = -\frac{\hbar}{q}\nabla\times(\nabla\times\varphi) \equiv \mp\Phi_0\delta_2(\boldsymbol{\rho}), \qquad \text{at } \rho >> \xi, \tag{6.64}$$

which coincides with Eq. (56) at all regular points $\rho \neq 0$. Spelling out the Laplace operator for our current case of axial symmetry,[36] we get an ordinary differential equation,

$$\delta_L^2\frac{1}{\rho}\frac{d}{d\rho}\left(\rho\frac{dB}{d\rho}\right) - B = 0, \qquad \text{for } \rho \neq 0. \tag{6.65}$$

Comparing this equation with Eq. (2.155) with $\nu = 0$, and taking into account that we need the solution decreasing at $\rho \to \infty$, making any contribution proportional to the function I_0 unacceptable, we get

[35] This equation was derived by Vitaly Lazarevich Ginzburg and Lev Davidovich Landau from phenomenological arguments in 1950, i.e. before the advent of the "microscopic" BSC theory, and may be used for simple analyses of a broad range of nonlinear effects in superconductors. The Ginzburg-Landau and Gross-Pitaevskii equations will be further discussed in SM Sec. 4.3.

[36] See, e.g., MA Eq. (10.3) with $\partial/\partial\varphi = \partial/\partial z = 0$.

$$B = CK_0\left(\frac{\rho}{\delta_L}\right) \tag{6.66}$$

– see the plot of this Bessel function on the right panel of Fig. 2.22 (black line). The constant C should be calculated by fitting the 2D delta function on the right-hand side of Eq. (64), i.e. by requiring

$$\int_{\text{vortex}} B(\rho)d^2\rho \equiv 2\pi\int_0^\infty B(\rho)\rho d\rho \equiv 2\pi\delta_L^2 C\int_0^\infty K_0(\zeta)\zeta d\zeta = \mp\Phi_0 . \tag{6.67}$$

The last, dimensionless integral equals 1,[37] so finally

$$B(\rho) = \frac{\Phi_0}{2\pi\delta_L^2}K_0\left(\frac{\rho}{\delta_L}\right), \qquad \text{at } \rho >> \xi . \tag{6.68}$$

So the magnetic field of the vortex drops exponentially at distances ρ much larger than δ_L, and diverges at $\rho \to 0$ – see, e.g., the second of Eqs. (2.157). However, this divergence is very slow (logarithmic), and, as was repeatedly discussed in this series, is avoided by the account of virtually any other factor. In our current case, this factor is the decrease of $|\psi|^2$ to zero at $\rho \sim \xi$ (see Fig. 5), not taken into account in Eq. (68). As a result, we may estimate the field on the axis of the vortex as

$$B(0) \approx \frac{\Phi_0}{2\pi\delta_L^2}\ln\frac{\delta_L}{\xi}; \tag{6.69}$$

the exact (and much more involved) solution of the problem confirms this estimate with a minor correction: $\ln(\delta_L/\xi) \to \ln(\delta_L/\xi) - 0.28$, i.e. $\xi \to 1.3\xi$.

The current density distribution may be now calculated from the Maxwell equation $\nabla \times \mathbf{B} = \mu\mathbf{j}$, giving $\mathbf{j} = j(\rho)\mathbf{n}_\varphi$, with[38]

$$j(\rho) = -\frac{1}{\mu}\frac{\partial B}{\partial \rho} = -\frac{\Phi_0}{2\pi\mu\delta_L^2}\frac{\partial}{\partial\rho}K_0\left(\frac{\rho}{\delta_L}\right) \equiv \frac{\Phi_0}{2\pi\mu\delta_L^3}K_1\left(\frac{\rho}{\delta_L}\right), \qquad \text{at } \rho >> \xi , \tag{6.70}$$

where the same identity (2.158), with $J_n \to K_n$ and $n = 1$, was used. Now looking at Eqs. (2.157) and (2.158), with $n = 1$, we see that the supercurrent's density is exponentially low at $\rho >> \delta_L$ (thus outlining the vortex' periphery), and is proportional to $1/\rho$ within the broad range $\xi << \rho << \delta_L$. This rise of the current at $\rho \to 0$ (which could be readily predicted directly from Eq. (54) with $\nabla\varphi = \pm\mathbf{n}_\varphi/\rho$, and the $\mathbf{A}$-term negligible at $\rho << \delta_L$) is quenched at $\rho \sim \xi$ by a rapid drop of the factor $|\psi|^2$ in the same Eq. (54), i.e. by the suppression of the superconductivity near the axis (by the same supercurrent!) – see Fig. 5 again.

This structure of the Abrikosov vortex may be used to calculate, in a straightforward way, its energy per unit length (i.e. its linear tension)

[37] This fact follows, for example, from the integration of both sides of Eq. (2.143) (which is valid for any Bessel functions, including K_n) with $n = 1$, from 0 to ∞, and then using the asymptotic values given by Eqs. (2.157)-(2.158): $K_1(\infty) = 0$, and $K_1(\zeta) \to 1/\zeta$ at $\zeta \to 0$.

[38] See, e.g., MA Eq. (10.5), with $f_\rho = f_\varphi = 0$, and $f_z = B(\rho)$.

$$\mathcal{T} \equiv \frac{U}{l} \approx \frac{\Phi_0^2}{4\pi\mu\delta_L^2} \ln\frac{\delta_L}{\xi}, \tag{6.71}$$

and hence the so-called "first critical" value H_{c1} of the external magnetic field,[39] at which the vortex formation becomes possible (in a long cylindrical sample parallel to the field):

$$H_{c1} = \frac{\mathcal{T}}{\Phi_0} \approx \frac{\Phi_0}{4\pi\mu\delta_L^2} \ln\frac{\delta_L}{\xi}. \tag{6.72}$$

Let me leave the proof of these two formulas for the reader's exercise.

The flux quantization and the Abrikosov vortices discussed above are just two of several *macroscopic quantum effects* in superconductivity. Let me discuss just one more, but perhaps the most interesting of such effects. Let us consider a superconducting ring/loop interrupted with a very narrow slit (Fig. 4b). Integrating Eq. (54) along any current-free path from point 1 to point 2 (see, e.g., dashed line in Fig. 4b), we get

$$0 = \int_1^2 \left(\nabla\varphi - \frac{q}{\hbar}\mathbf{A}\right)\cdot d\mathbf{r} = \varphi_2 - \varphi_1 - \frac{q}{\hbar}\Phi. \tag{6.73}$$

Using the flux quantum definition (62), this result may be rewritten as

$$\varphi \equiv \varphi_1 - \varphi_2 = \frac{2\pi}{\Phi_0}\Phi, \tag{6.74}$$

Josephson phase difference

where φ is called the *Josephson phase difference*. Note that in contrast to each of the phases $\varphi_{1,2}$, their difference φ is gauge-invariant: Eq. (74) directly relates it to the gauge-invariant magnetic flux Φ.

Can this φ be measured? Yes, for example, using the *Josephson effect*.[40] Let us consider two (for the argument simplicity, similar) superconductors, connected with some sort of *weak link*, for example, a small tunnel junction, or a point contact, or a narrow thin-film bridge, through which a weak Cooper-pair supercurrent can flow. (Such a system of two weakly coupled superconductors is called a *Josephson junction*.) Let us think about what this supercurrent I may be a function of. For that, reverse thinking is helpful: let us imagine that we change the current; what parameter of the superconducting condensate can it affect? If the current is very weak, it cannot perturb the superconducting condensate's density, proportional to $|\psi|^2$; hence it may only change the Cooper condensate phases $\varphi_{1,2}$. However, according to Eq. (53), the phases are not gauge-invariant, while the current should be. Hence the current may affect (or, if you like, may be affected by) only the phase difference φ defined by Eq. (74). Moreover, just has already been argued during the flux quantization discussion, a change of any of $\varphi_{1,2}$ (and hence of φ) by 2π or any of its multiples should not change the current. Also, if the wavefunction is the same in both superconductors ($\varphi = 0$), the supercurrent should vanish due to the system's symmetry. Hence the function $I(\varphi)$ should satisfy the following conditions:

[39] This term is used to distinguish H_{c1} from the higher "second critical field" H_{c2}, at which the Abrikosov vortices are pressed to each other so tightly (to distances $d \sim \xi$) that they merge, and the remains of superconductivity vanish: $\psi \to 0$. Unfortunately, I do not have time/space to discuss these effects; the interested reader may be referred, for example, to Chapter 5 of M. Tinkham's monograph cited above.

[40] It was predicted in 1961 by Brian David Josephson (then a PhD student!) and observed experimentally by several groups soon after that.

$$I(0) = 0, \qquad I(\varphi + 2\pi) = I(\varphi). \tag{6.75}$$

With these conditions on hand, we should not be terribly surprised by the following Josephson's result that for the weak link provided by tunneling,[41]

Josephson (super)current

$$\boxed{I(\varphi) = I_c \sin\varphi}, \tag{6.76}$$

where constant I_c, which depends on the weak link's strength and temperature, is called the *critical current*. Actually, Eqs. (54) and (63) enable not only a straightforward calculation of this relation but even obtaining a simple expression of the critical current I_c via the link's normal-sate resistance – the task left for the (creative :-) reader's exercise.

Now let us see what happens if a Josephson junction is placed into the gap in a superconductor loop – see Fig. 4c. In this case, we may combine Eqs. (74) and (76), getting

Macroscopic quantum interference

$$\boxed{I = I_c \sin\left(2\pi \frac{\Phi}{\Phi_0}\right)}. \tag{6.77}$$

This effect of a periodic dependence of the current on the magnetic flux is called *macroscopic quantum interference*,[42] while the system shown in Fig. 4c, the *superconducting quantum interference device – SQUID* (with all letters capitalized, please :-). The low value of the magnetic flux quantum Φ_0, and hence the high sensitivity of φ to external magnetic fields, allows using such SQUIDs as ultrasensitive magnetometers. Indeed, for a superconducting ring of area ~1 cm^2, one period of the change of the supercurrent (77) is produced by a magnetic field change of the order of 10^{-11} T (10^{-7} Gs), while sensitive electronics allows measuring a tiny fraction of this period – limited by thermal noise at a level of the order of a few fT. Such sensitivity allows measurements, for example, of the miniscule magnetic fields induced outside of the body by the beating human heart, and even by brain activity.[43]

An important aspect of quantum interference is the so-called *Aharonov-Bohm* (AB) *effect* – which actually takes place for single quantum particles as well.[44] Let the magnetic field lines be limited to the central, hollow part of the SQUID loop so that no appreciable magnetic field ever touches the ring itself. (This may be done experimentally with very good accuracy, for example using high-μ magnetic cores – see their discussion in Sec. 5.6.) As predicted by Eq. (77), and confirmed by several careful experiments carried out in the mid-1960s,[45] this restriction does not matter – the interference is observed

[41] For some other types of weak links, the function $I(\varphi)$ may deviate from the sinusoidal form Eq. (76) rather considerably, while still satisfying the general conditions (75).

[42] The name is due to a deep analogy between this phenomenon and the interference between two coherent waves, to be discussed in detail in Sec. 8.4.

[43] Other practical uses of SQUIDs include MRI signal detectors, high-sensitive measurements of magnetic properties of materials, and weak field detection in a broad variety of physical experiments – see, e.g., J. Clarke and A. Braginski (eds.), *The SQUID Handbook*, vol. II, Wiley, 2006. For a comparison of these devices with other sensitive magnetometers see, e.g., the review collection by A. Grosz *et al.* (eds.), *High Sensitivity Magnetometers*, Springer, 2017.

[44] For a more detailed discussion of the AB effect see, e.g., QM Sec. 3.2.

[45] Similar experiments have been carried out with single (unpaired) electrons – moving either ballistically, in vacuum, or in "normal" (non-superconducting) conducting rings. In the last case, the effect is much harder to observe than in SQUIDs: the ring size has to be very small, and temperature very low, to avoid the so-called

anyway. This means that not only the magnetic field **B** but also the vector potential **A** represents physical reality, albeit in a quite peculiar way – remember the gauge transformation (5.46), which you may carry out in your head, without changing any physical reality? (Fortunately, this transformation does not change the contour integral participating in Eq. (5.65), and hence the magnetic flux Φ, and hence the interference pattern.)

Actually, the magnetic flux quantization (62) and the macroscopic quantum interference (77) are not completely different effects, but just two manifestations of the interrelated macroscopic quantum phenomena. To show that, one should note that if the critical current I_c (or rather its product by the loop's self-inductance L) is high enough, the flux Φ in the SQUID loop is due not only to the external magnetic field flux Φ_{ext} but also has a self-field component – cf. Eq. (5.68):[46]

$$\Phi = \Phi_{ext} - LI, \qquad \text{where } \Phi_{ext} \equiv \int_S (B_{ext})_n d^2 r . \tag{6.78}$$

Now the relation between Φ and Φ_{ext} may be readily found by solving this equation together with Eq. (77). Figure 6 shows this relation for several values of the dimensionless parameter $\lambda \equiv 2\pi LI_c/\Phi_0$.

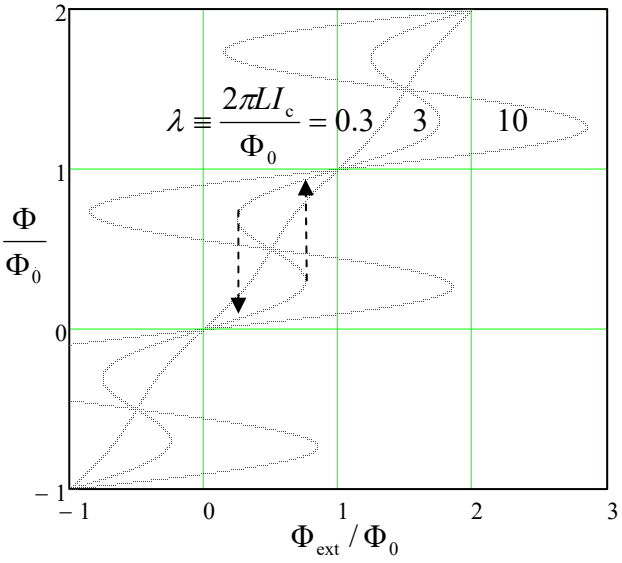

Fig. 6.6. The function $\Phi(\Phi_{ext})$ for SQUIDs with various values of the normalized LI_c product. Dashed arrows show the flux leaps as the external field is changed. (The branches with $d\Phi/d\Phi_{ext} < 0$ are unstable.)

These plots show that if the critical current (and/or the inductance) is low, $\lambda << 1$, the self-field effects are negligible, and the total flux follows the external field (i.e., Φ_{ext}) faithfully. However, at $\lambda > 1$, the function $\Phi(\Phi_{ext})$ becomes hysteretic, and at $\lambda >> 1$, its stable (positive-slope) branches are nearly flat, with the total flux values corresponding to Eq. (62). Thus, a superconducting ring closed with a high-I_c Josephson junction exhibits a nearly-perfect flux quantization.

The self-field effects described by Eq. (78) create certain technical problems for SQUID magnetometry, but they are the basis for one more useful application of these devices: ultrafast

dephasing effects due to unavoidable interactions of the electrons with their environment – see, e.g., QM Chapter 7.

[46] The sign before *LI* would be positive, as in Eq. (5.70), if *I* was the current flowing *into* the inductance. However, in order to keep the sign in Eq. (76) intact, *I* should mean the current flowing into the Josephson junction, i.e. *from* the inductance, thus changing the sign of the *LI* term in Eq. (78).

computing. Indeed, Fig. 6 shows that at the values of λ modestly above 1 (e.g., $\lambda \approx 3$), and within a certain range of applied field, the SQUID has two stable flux states, which differ by $\Delta\Phi \approx \Phi_0$ and may be used for coding binary 0 and 1. For practical superconductors (like Nb), the time of switching between these states (see dashed arrows in Fig. 4) is of the order of a picosecond, while the energy dissipated at such event may be as low as $\sim 10^{-19}$ J. (This bound is determined not by device's physics, by the fundamental requirement for the energy barrier between the two states to be much higher than the thermal fluctuation energy scale $k_B T$, ensuring a sufficiently long information retention time.) While the picosecond switching speed may be also achieved with some semiconductor devices, the power consumption of the SQUID-based digital devices may be 5 to 6 orders of magnitude lower, enabling large-scale digital integrated circuits with 100-GHz-scale clock frequencies. Unfortunately, the range of practical applications of these *Rapid Single-Flux-Quantum* (RSFQ) digital circuits is still very narrow, due to the inconvenience of their deep refrigeration to temperatures below T_c.[47]

Since we have already got the basic relations (74) and (76) describing the macroscopic quantum phenomena in superconductivity, let me mention in brief two other prominent members of this group, called the *dc* and *ac Josephson effects*. Differentiating Eq. (74) over time, and using the Faraday induction law (2), we get[48]

Josephson phase-to-voltage relation

$$\frac{d\varphi}{dt} = \frac{2e}{\hbar} V . \tag{6.79}$$

This famous *Josephson phase-to-voltage relation* should be valid regardless of the way how the voltage V has been created,[49] so let us apply Eqs. (76) and (79) to the simplest circuit with a non-superconducting source of dc voltage – see Fig. 7.

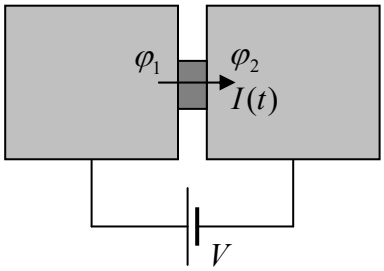

Fig. 6.7. DC-voltage-biased Josephson junction.

If the current's magnitude is below the critical value, Eq. (76) allows phase φ to have the time-independent value

$$\varphi = \sin^{-1}\frac{I}{I_c}, \qquad \text{if } -I_c < I < +I_c , \tag{6.80}$$

and hence, according to Eq. (79), a vanishing voltage drop across the junction: $V = 0$. This *dc Josephson effect* is not quite surprising – indeed, we have postulated from the very beginning that the Josephson junction may pass a certain supercurrent. Much more fascinating is the so-called *ac Josephson effect* that occurs if the voltage across the junction has a non-zero average (dc) component V_0. For simplicity, let us

[47] For more on that technology, see, e.g., the review paper by P. Bunyk *et al.*, *Int. J. High Speed Electron. Syst.* **11**, 257 (2001), and references therein.

[48] Since the induced e.m.f. $\mathcal{V}_{ind}$ cannot drop on the superconducting path between the Josephson junction electrodes 1 and 2 (see Fig. 4c), it should be equal to $(-V)$, where V is the voltage across the junction.

[49] Indeed, it may be also obtained from simple Schrödinger-equation-based arguments – see, e.g., QM Sec. 1.6.

assume that this is the *only* voltage component: $V(t) = V_0 = \text{const}$;[50] then Eq. (79) may be easily integrated to give $\varphi = \omega_J t + \varphi_0$, where

$$\omega_J \equiv \frac{2e}{\hbar} V_0 . \tag{6.81}$$

Josephson oscillation frequency

This result, plugged into Eq. (76), shows that the supercurrent oscillates,

$$I = I_c \sin\left(\omega_J t + \varphi_0\right), \tag{6.82}$$

with the so-called *Josephson frequency* ω_J (81) proportional to the applied dc voltage. For practicable voltages (above the typical noise level), the frequency $f_J = \omega_J/2\pi$ corresponds to the GHz or even THz ranges, because the proportionality coefficient in Eq. (81) is very high: $f_J/V_0 = e/\pi\hbar \approx 483$ MHz/μV.[51]

An important experimental fact is the universality of this coefficient. For example, in the mid-1980s, a Stony Brook group led by J. Lukens proved that this factor is material-independent with a relative accuracy of at least 10^{-15}. Very few experiments, especially in solid-state physics, have ever reached such precision. This fundamental nature of the Josephson voltage-to-frequency relation (81) allows an important application of the ac Josephson effect in metrology. Namely, phase-locking[52] the Josephson oscillations with an external microwave signal from an atomic frequency standard, one can get a more precise dc voltage than from any other source. In NIST and other metrological institutions around the globe, this effect is used for the calibration of simpler "secondary" voltage standards that can operate at room temperature.

6.6. Inductors, transformers, and ac Kirchhoff laws

Let a *wire coil* (meaning either a single loop illustrated in Fig. 5.4b or a series of such loops, such as one of the solenoids shown in Fig. 5.6) have a self-inductance L much larger than that of the wires connecting it to other components of our system: ac voltage sources, voltmeters, etc. (Since, according to Eq. (5.75), L scales as the square of the number N of wire turns, this condition is easier to satisfy at $N >> 1$.) Then in a quasistatic system consisting of such *lumped induction coils*, external wires, and other lumped circuit elements such as resistors, capacitances, etc., we may neglect the electromagnetic induction effects everywhere outside the coil, so the electric field in those external regions is potential. Then the voltage V between the coil's terminals may be defined, just as in electrostatics, as the difference of values of ϕ between the terminals, i.e. as the integral

$$V = \int \mathbf{E} \cdot d\mathbf{r} \tag{6.83}$$

between the coil terminals along any path outside the coil. This voltage has to be balanced by the induction e.m.f. (2) in the coil, so if the Ohmic resistance of the coil is negligible, we may write

[50] In experiment, this condition is hard to implement, due to the relatively high inductances of the current leads providing the dc voltage supply. However, this technical complication does not affect the main conclusion of the simple analysis described here.

[51] This 1962 prediction (by the same B. Josephson) was confirmed experimentally – in 1963 indirectly, by phase-locking of the oscillations (82) with an external microwave signal, and in 1967 explicitly, by the direct detection of the emitted microwave radiation.

[52] For a discussion of this very important (and general) effect, see, e.g., CM Sec. 5.4.

$$V = \frac{d\Phi}{dt}, \tag{6.84}$$

where Φ is the magnetic flux in the coil.[53] If the flux is due to the current I in the same coil only (i.e. if it is magnetically uncoupled from other coils), we may use Eq. (5.70) to get the well-known relation

Voltage drop on inductance coil

$$V = L\frac{dI}{dt}, \tag{6.85}$$

where compliance with the Lenz sign rule is achieved by selecting the relations between the assumed voltage polarity and the current direction as shown in Fig. 8a.

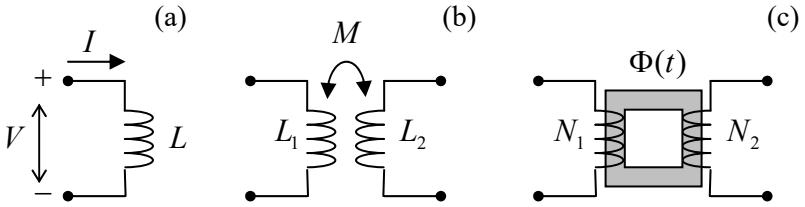

Fig. 6.8. Some lumped ac circuit elements: (a) an induction coil, (b) two inductively coupled coils, and (c) an ac transformer.

If similar conditions are satisfied for two magnetically coupled coils (Fig. 8b), then, in Eq. (84), we need to use Eqs. (5.69) instead, getting

$$V_1 = L_1\frac{dI_1}{dt} + M\frac{dI_2}{dt}, \qquad V_2 = L_2\frac{dI_2}{dt} + M\frac{dI_1}{dt}. \tag{6.86}$$

Such systems of inductively coupled coils have numerous applications in electrical engineering and physical experiment. Perhaps the most important of them is the *ac transformer*, in which the coils share a common soft-ferromagnetic core of the toroidal ("doughnut") topology – see Fig. 8c.[54] As we already know from the discussion in Sec. 5.6, such cores, with $\mu >> \mu_0$, "try" to absorb all magnetic field lines, so the magnetic flux $\Phi(t)$ in the core is nearly the same in each of its cross-sections. With this, Eq. (84) yields

$$V_1 \approx N_1\frac{d\Phi}{dt}, \quad V_2 \approx N_2\frac{d\Phi}{dt}, \tag{6.87}$$

so the voltage ratio is completely determined by the ratio N_1/N_2 of the number of wire turns.

Now we may generalize, to the ac current case, the Kirchhoff laws already discussed in Sec. 4.1 – see Fig. 4.3 reproduced in Fig. 9a below. Let not only inductances but also capacitances and resistances of the wires be negligible in comparison with those of the lumped (compact) circuit elements, whose list now would include not only resistors and current sources (as in the dc case), but also the induction coils (including magnetically coupled ones) and capacitors – see Fig. 9b. In the quasistatic approximation, the current flowing in each wire is conserved, so the "node rule", i.e. the 1st Kirchhoff law (4.7a),

[53] If the resistance is substantial, it may be represented by a separate lumped circuit element (resistor) connected in series with the coil.

[54] The first practically acceptable form of this device, called the *Stanley transformer*, was invented in 1886. In it, multi-turn windings could be easily mounted onto a toroidal ferromagnetic (at that time, silicon-steel-plate) core.

$$\sum_j I_j = 0 . \tag{6.88a}$$

remains valid. Also, if the electromagnetic induction effect is restricted to the interior of lumped induction coils as discussed above, the voltage drops V_k across each circuit element may be still represented, just as in dc circuits, with differences between the adjacent node potentials. As a result, the "loop rule", i.e. 2nd Kirchhoff law (4.7b),

$$\sum_k V_k = 0 , \tag{6.88b}$$

is also valid. Now, in contrast to the dc case, Eqs. (88) may be the (ordinary) differential equations. However, if all circuit elements are linear (as in the examples presented in Fig. 9b), these equations may be readily reduced to linear algebraic equations, using the Fourier expansion. (In the common case of sinusoidal ac sources, the final stage of the Fourier series summation is unnecessary.)

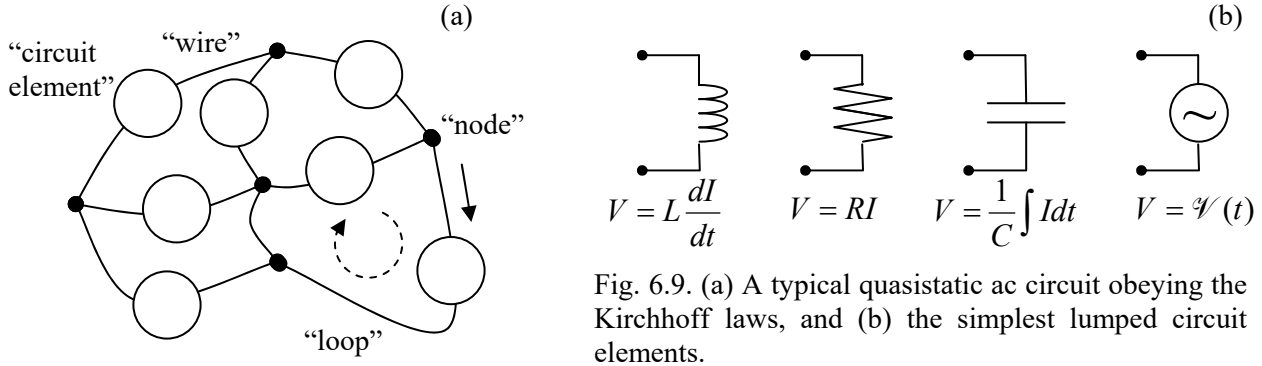

Fig. 6.9. (a) A typical quasistatic ac circuit obeying the Kirchhoff laws, and (b) the simplest lumped circuit elements.

My teaching experience shows that the potential readers of these notes are well familiar with the application of Eqs. (88) to such problems from their undergraduate studies, so I will save time/space by skipping discussions of even the simplest examples of such circuits, such as *LC*, *LR*, *RC*, and *LRC* loops and periodic structures.[55] However, since such problems are very important for practice, my sincere advice to the reader is to carry out a self-test by solving a few problems of this type, provided in Sec. 9 below, and if they cause any difficulty, pursue some remedial reading.

6.7. Displacement currents

Electromagnetic induction is not the only new effect arising in non-stationary electrodynamics. Indeed, though Eqs. (21) are adequate for the description of quasistatic phenomena, a deeper analysis shows that one of these equations, namely $\nabla \times \mathbf{H} = \mathbf{j}$, cannot be exact. To see that, let us take the divergence of both sides:

$$\nabla \cdot (\nabla \times \mathbf{H}) = \nabla \cdot \mathbf{j} . \tag{6.89}$$

But, as the divergence of any curl,[56] the left-hand side should equal zero. Hence we get

[55] Curiously enough, these effects include wave propagation in periodic *LC* circuits, even within the quasistatic approximation! However, the speed $1/(LC)^{1/2}$ of these waves in lumped circuits is much lower than the speed $1/(\varepsilon\mu)^{1/2}$ of electromagnetic waves in the surrounding medium – see Sec. 8 below.

[56] Again, see MA Eq. (11.2) – if you need it.

$$\nabla \cdot \mathbf{j} = 0 . \tag{6.90}$$

This is fine in statics, but in dynamics, this equation forbids any charge accumulation, because according to the continuity relation (4.5),

$$\nabla \cdot \mathbf{j} = -\frac{\partial \rho}{\partial t} . \tag{6.91}$$

This discrepancy had been recognized by James Clerk Maxwell who suggested, in the 1860s, a way out of this contradiction. If we generalize the equation for $\nabla \times \mathbf{H}$ by adding to the term $\mathbf{j}$ (that describes the density of real electric currents) the so-called *displacement current* density term,

Displacement current density

$$\boxed{\mathbf{j}_{\mathrm{d}} \equiv \frac{\partial \mathbf{D}}{\partial t}}, \tag{6.92}$$

(which of course vanishes in statics), then the equation takes the form

$$\nabla \times \mathbf{H} = \mathbf{j} + \mathbf{j}_{\mathrm{d}} \equiv \mathbf{j} + \frac{\partial \mathbf{D}}{\partial t} . \tag{6.93}$$

In this case, due to the equation (3.22), $\nabla \cdot \mathbf{D} = \rho$, the divergence of the right-hand side equals zero due to the continuity equation (92), and the discrepancy is removed. This incredible theoretical feat,[57] confirmed by the 1886 experiments carried out by Heinrich Hertz (see below) was perhaps the main triumph of theoretical physics of the 19th century.

Maxwell's displacement current concept, expressed by Eq. (93), is so important that it is worthwhile to have one more look at its derivation using a particular model shown in Fig. 10.[58]

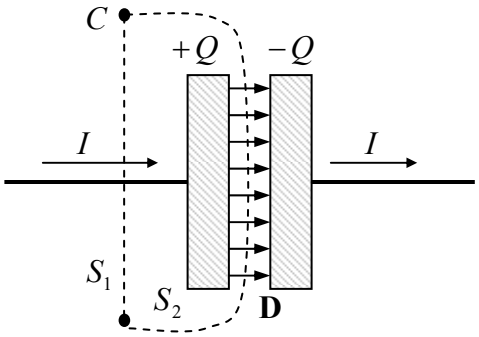

Fig. 6.10. The Ampère law applied to capacitor recharging.

Neglecting the fringe field effects, we may use Eq. (4.1) to describe the relationship between the current I flowing through the wires and the electric charge Q of the capacitor:[59]

$$\frac{dQ}{dt} = I . \tag{6.94}$$

[57] It looks deceivingly simple now – after the fact, and with the current mathematical tools (especially the del operator), which are much superior to those that were available to J. Maxwell.

[58] No physicist should be ashamed of doing this. For example, J. Maxwell's main book, *A Treatise of Electricity and Magnetism*, is full of drawings of plane capacitors, inductance coils, and voltmeters. More generally, the whole history of science teaches us that snobbery regarding particular examples and practical systems is a virtually certain path toward producing nothing of either practical value or fundamental importance.

[59] This is of course just the integral form of the continuity equation (91).

Now let us consider a closed contour C drawn around the wire. (Solid points in Fig. 10 show the places where the contour intercepts the plane of the drawing.) This contour may be seen as the line limiting either surface S_1 (crossed by the wire) or surface S_2 (avoiding such crossing by passing through the capacitor's gap). Applying the macroscopic Ampère law (5.116) to the former surface, we get

$$\oint_C \mathbf{H}\cdot d\mathbf{r} = \int_{S_1} j_n d^2r = I, \tag{6.95}$$

while for the latter surface the same law gives a different result,

$$\oint_C \mathbf{H}\cdot d\mathbf{r} = \int_{S_2} j_n d^2r = 0, \qquad \text{[WRONG!]} \tag{6.96}$$

for the same integral. This is just an integral-form manifestation of the discrepancy outlined above, but it shows clearly how serious the problem is (or rather it was – before Maxwell).

Now let us see how the introduction of the displacement currents saves the day, considering for the sake of simplicity a plane capacitor of area A, with a small and constant electrode spacing. In this case, as we already know, the field inside it is uniform, with $D = \sigma$, so the total capacitor's charge $Q = A\sigma = AD$, and the current (94) may be represented as

$$I = \frac{dQ}{dt} = A\frac{dD}{dt}. \tag{6.97}$$

So, instead of the wrong Eq. (96), the Ampère law modified following Eq. (93), gives

$$\oint_C \mathbf{H}\cdot d\mathbf{r} = \int_{S_2} (j_{\text{d}})_n d^2r = \int_{S_2} \frac{\partial D_n}{\partial t} d^2r = \frac{dD}{dt} A = I, \tag{6.98}$$

i.e. the Ampère integral becomes independent of the choice of the surface limited by the contour C – as it has to be.

6.8. Finally, the full Maxwell equation system

. This is a very special moment in this course: with the displacement currents in, i.e. with the replacement of Eq. (5.107) with Eq. (93), we have finally arrived at the full set of macroscopic Maxwell equations for time-dependent fields,[60]

$$\nabla\times\mathbf{E} + \frac{\partial\mathbf{B}}{\partial t} = 0, \qquad \nabla\times\mathbf{H} - \frac{\partial\mathbf{D}}{\partial t} = \mathbf{j}, \tag{6.99a}$$

$$\nabla\cdot\mathbf{D} = \rho, \qquad \nabla\cdot\mathbf{B} = 0, \tag{6.99b}$$

Macroscopic Maxwell equations

whose validity has been confirmed by an enormous body of experimental data. Indeed, despite numerous efforts, no other corrections (e.g., additional terms) to the Maxwell equations have been ever found, and these equations are still considered exact within the range of their validity, i.e. while the electric and magnetic fields may be considered classically. Moreover, even in quantum theory, these

[60] This vector form of the Maxwell equations, magnificent in its symmetry and simplicity, was developed in 1884-85 by Oliver Heaviside, with substantial contributions by H. Lorentz. (The original Maxwell's result circa 1864 looked like a system of 20 equations for Cartesian components of the vector and scalar potentials.)

equations are believed to be *strictly* valid as relations between the Heisenberg operators of the electric and magnetic fields.[61] (Note that the *microscopic* Maxwell equations for the genuine fields **E** and **B** may be formally obtained from Eqs. (99) by the substitutions $\mathbf{D} = \varepsilon_0\mathbf{E}$ and $\mathbf{H} = \mathbf{B}/\mu_0$, and the simultaneous replacement of the stand-alone charge and current densities on their right-hand sides with the full ones.)

Perhaps the most striking feature of these equations is that, even in the absence of stand-alone charges and currents inside the region of our interest, when the equations become fully homogeneous,

$$\nabla\times\mathbf{E} = -\frac{\partial\mathbf{B}}{\partial t}, \qquad \nabla\times\mathbf{H} = \frac{\partial\mathbf{D}}{\partial t}, \tag{6.100a}$$

$$\nabla\cdot\mathbf{D} = 0, \qquad \nabla\cdot\mathbf{B} = 0, \tag{6.100b}$$

they still describe something very non-trivial: *electromagnetic waves*, including light. The physics of the waves may be clearly seen from Eqs. (100a): according to the first of them, the change of the magnetic field in time creates a vortex-like (divergence-free) electric field. On the other hand, the second of Eqs. (100a) describes how the changing electric field, in turn, creates a vortex-like magnetic field. So-coupled electric and magnetic fields may propagate as waves – even very far from their sources.

We will carry out a detailed quantitative analysis of the waves in the next chapter, and here I will only use this notion to make good on the promise given in Sec. 3, namely to establish the condition of validity of the quasistatic approximation (21). For simplicity, let us consider an electromagnetic wave with a time period $\mathcal{T}$, velocity v, and hence the wavelength[62] $\lambda = v\mathcal{T}$ in a linear medium with $\mathbf{D} = \varepsilon\mathbf{E}$, $\mathbf{B} = \mu\mathbf{H}$. Then the magnitude of the left-hand side of the first of Eqs. (100a) is of the order of $E/\lambda = E/v\mathcal{T}$, while that of its right-hand side may be estimated as $B/\mathcal{T} \sim \mu H/\mathcal{T}$. Using similar estimates for the second of Eqs. (100a), we arrive at the following two requirements:[63]

$$\frac{E}{H} \sim \mu v \sim \frac{1}{\varepsilon v}. \tag{6.101}$$

To ensure the compatibility of these two relations, the wave's speed should satisfy the estimate

$$v \sim \frac{1}{(\varepsilon\mu)^{1/2}}, \tag{6.102}$$

reduced to $v \sim 1/(\varepsilon_0\mu_0)^{1/2} \equiv c$ in free space, while the ratio of the electric and magnetic field amplitudes should be of the following order:

$$\frac{E}{H} \sim \mu v \sim \mu\frac{1}{(\varepsilon\mu)^{1/2}} \equiv \left(\frac{\mu}{\varepsilon}\right)^{1/2}. \tag{6.103}$$

(In the next chapter we will see that for plane electromagnetic waves, these results are exact.)

Now, let a system of a linear size $\sim a$ carry currents producing a certain magnetic field H. Then, according to Eqs. (100a), their magnetic field Faraday-induces the electric field of magnitude $E \sim \mu Ha/\mathcal{T}$, whose displacement currents, in turn, produce an additional magnetic field with magnitude

[61] See, e.g., QM Chapter 9.

[62] Let me hope the reader knows that the relation $\lambda = v\mathcal{T}$ is universal and valid for waves of any nature – see, e.g., CM Chapter 6. (In the case of substantial dispersion, v means the phase velocity.)

[63] The fact that $\mathcal{T}$ has canceled, shows that these estimates are valid for waves of any frequency.

$$H' \sim \frac{a\varepsilon}{\mathcal{T}} E \sim \frac{a\varepsilon}{\mathcal{T}} \frac{\mu a}{\mathcal{T}} H \equiv \left(\frac{a\lambda}{v\mathcal{T}\lambda} \right)^2 H \equiv \left(\frac{a}{\lambda} \right)^2 H . \tag{6.104}$$

Hence, the displacement current effects are negligible for a system of size $a << \lambda$.[64]

In particular, the quasistatic picture of the skin effect, discussed in Sec. 3, is valid while the skin depth (33) remains much *smaller* than the corresponding wavelength,

$$\lambda = v\mathcal{T} = \frac{2\pi v}{\omega} = \left(\frac{4\pi^2}{\varepsilon\mu\omega^2} \right)^{1/2} . \tag{6.105}$$

The wavelength decreases with the frequency as $1/\omega$, i.e. faster than $\delta_s \propto 1/\omega^{1/2}$, so they become comparable at the crossover frequency

$$\omega_r = \frac{\sigma}{\varepsilon} \equiv \frac{\sigma}{\kappa\varepsilon_0}, \tag{6.106}$$

which is nothing else than the reciprocal charge relaxation time (4.10). As was discussed in Sec. 4.2, for good metals this frequency is extremely high (about 10^{18} s^{-1}), so the validity of Eq. (33) is typically limited by the anomalous skin effect (which was briefly discussed in Sec. 3), rather than the wave effects.

Before going after the analysis of the full Maxwell equations for particular situations (that will be the main goal of the next chapters of this course), let us have a look at the energy balance they yield for a certain volume V, which may include both some charged particles and the electromagnetic field. Since, according to Eq. (5.10), the magnetic field performs no work on charged particles even if they move, the total power $\mathscr{P}$ being transferred from the field to the particles inside the volume is due to the electric field alone – see Eq. (4.38):

$$\mathscr{P} = \int_V \mathscr{p}\, d^3r, \qquad \text{with } \mathscr{p} = \mathbf{j}\cdot\mathbf{E}, \tag{6.107}$$

Expressing **j** from the corresponding Maxwell equation of the system (99), we get

$$\mathscr{P} = \int_V \left[\mathbf{E}\cdot(\nabla\times\mathbf{H}) - \mathbf{E}\cdot\frac{\partial\mathbf{D}}{\partial t} \right] d^3r. \tag{6.108}$$

Let us pause here for a second, and transform the divergence of **E**×**H**, using the well-known vector algebra identity:[65]

$$\nabla\cdot(\mathbf{E}\times\mathbf{H}) = \mathbf{H}\cdot(\nabla\times\mathbf{E}) - \mathbf{E}\cdot(\nabla\times\mathbf{H}). \tag{6.109}$$

The last term on the right-hand side of this equality is exactly the first term in the square brackets of Eq. (108), so we may rewrite that formula as

$$\mathscr{P} = \int_V \left[-\nabla\cdot(\mathbf{E}\times\mathbf{H}) + \mathbf{H}\cdot(\nabla\times\mathbf{E}) - \mathbf{E}\cdot\frac{\partial\mathbf{D}}{\partial t} \right] d^3r. \tag{6.110}$$

[64] Let me emphasize that if this condition is *not* fulfilled, the lumped-circuit representation of the system (see Fig. 9 and its discussion) is typically inadequate – besides some special cases, to be discussed in the next chapter.

[65] See, e.g., MA Eq. (11.7) with **f** = **E** and **g** = **H**.

However, according to the Maxwell equation for $\nabla \times \mathbf{E}$, this curl is equal to $-\partial\mathbf{B}/\partial t$, so the second term in the square brackets of Eq. (110) equals $-\mathbf{H}\cdot\partial\mathbf{B}/\partial t$ and, according to Eq. (14), is just the (minus) time derivative of the magnetic energy per unit volume. Similarly, according to Eq. (3.76), the third term under the integral is the (minus) time derivative of the electric energy per unit volume. Finally, we can use the divergence theorem to transform the integral of the first term in the square brackets to a 2D integral over the surface S limiting the volume V. As a result, we get the so-called *Poynting theorem*[66] for the power balance in the system:

Poynting theorem

$$\int_V \left(\mathcal{P} + \frac{\partial u}{\partial t} \right) d^3 r + \oint_S S_n d^2 r = 0 . \tag{6.111}$$

Here u is the density of the total (electric plus magnetic) energy of the electromagnetic field, with

Field's energy variation

$$\delta u \equiv \mathbf{E} \cdot \delta\mathbf{D} + \mathbf{H} \cdot \delta\mathbf{B} \tag{6.112}$$

– just the sum of the expressions given by Eqs. (3.76) and (14). For the particular case of an isotropic, linear, and dispersion-free medium, with $\mathbf{D}(t) = \varepsilon\mathbf{E}(t)$, $\mathbf{B}(t) = \mu\mathbf{H}(t)$, Eq. (112) yields

Field's energy

$$u = \frac{\mathbf{E}\cdot\mathbf{D}}{2} + \frac{\mathbf{H}\cdot\mathbf{B}}{2} \equiv \frac{\varepsilon E^2}{2} + \frac{B^2}{2\mu} . \tag{6.113}$$

Another key notion participating in Eq. (111) is the *Poynting vector*, defined as[67]

Poynting vector

$$\mathbf{S} \equiv \mathbf{E} \times \mathbf{H} . \tag{6.114}$$

The first integral in Eq. (111) is evidently the net change of the energy of the system (particles + field) per unit time, so the second (surface) integral has to be the power flowing out from the system through the surface. As a result, it is tempting to interpret the Poynting vector **S** locally, as the power flow density at the given point. In many cases, such a local interpretation of vector **S** is legitimate; however, in other cases, it may lead to wrong conclusions. Indeed, let us consider the simple system shown in Fig. 11: a charged plane capacitor placed into a static and uniform external magnetic field, so that the electric and magnetic fields are mutually perpendicular.

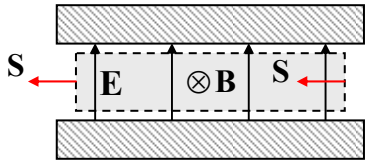

Fig. 6.11. The Poynting vector paradox.

In this static situation, with no charges moving, both $\mathcal{P}$ and $\partial/\partial t$ are equal to zero, and there should be no power flow in the system. However, Eq. (114) shows that the Poynting vector is not equal

[66] It is named after John Henry Poynting for his work published in 1884, though this fact was independently discovered by O. Heaviside in 1885 in a simpler form, while a similar result for the intensity of mechanical elastic waves had been obtained earlier (in 1874) by Nikolay Alekseevich Umov – see, e.g., CM Sec. 7.7.

[67] Actually, an addition to **S** of the curl of an arbitrary vector function $\mathbf{f}(\mathbf{r}, t)$ does not change Eq. (111). Indeed, we may use the divergence theorem to transform the corresponding change of the surface integral in Eq. (111) to a volume integral of scalar function $\nabla\cdot(\nabla\times\mathbf{f})$ that equals zero at any point – see, e.g., MA Eq. (11.2).

to zero inside the capacitor, being directed as the red arrows in Fig. 11 show. From the point of view of the only unambiguous corollary of the Maxwell equations, Eq. (111), there is no contradiction here, because the fluxes of the vector **S** through the side boundaries of the volume shaded in Fig. 11 are equal and opposite (and they are zero for other faces of this rectilinear volume), so the total flux of the Poynting vector through the volume boundary equals zero, as it should. It is, however, useful to recall this example each time before giving a local interpretation of the vector **S**.

The paradox illustrated in Fig. 11 is closely related to the *radiation recoil effects*, due to the electromagnetic field's momentum – more exactly, it *linear momentum*. Indeed, acting as at the Poynting theorem derivation, it is straightforward to use the *microscopic* Maxwell equations[68] to prove that, neglecting the boundary effects, the vector sum of the mechanical linear momentum of the particles in an arbitrary volume, and the integral of the following vector,

$$\mathbf{g} \equiv \frac{\mathbf{S}}{c^2}, \tag{6.115}$$

Electro-magnetic field's momentum

over the same volume, is conserved, enabling an interpretation of **g** as the density of the linear momentum of the electromagnetic field. (It will be more convenient for me to prove this relation, and discuss the related issues, in Sec. 9.8, using the 4-vector formalism of special relativity.) Due to this conservation, if some static fields coupled to mechanical bodies are suddenly decoupled from them and are allowed to propagate in space, i.e. to change their local integral of **g**, they give the bodies an equal and opposite impulse of force.

Finally, to complete our initial discussion of the Maxwell equations,[69] let us rewrite them in terms of potentials **A** and ϕ, because this is more convenient for the solution of some (though not all!) problems. Even when dealing with the system (99) of the more general Maxwell equations than discussed before, Eqs. (7) are still used for the definition of the potentials. It is straightforward to verify that with these definitions, the two homogeneous Maxwell equations (99b) are satisfied automatically. Plugging Eqs. (7) into the inhomogeneous equations (99a), and considering, for simplicity, a linear, uniform medium with frequency-independent ε and μ, we get

$$\nabla^2\phi + \frac{\partial}{\partial t}(\nabla\cdot\mathbf{A}) = -\frac{\rho}{\varepsilon}, \qquad \nabla^2\mathbf{A} - \varepsilon\mu\frac{\partial^2\mathbf{A}}{\partial t^2} - \nabla\left(\nabla\cdot\mathbf{A} + \varepsilon\mu\frac{\partial\phi}{\partial t}\right) = -\mu\mathbf{j}. \tag{6.116}$$

This is a more complex result than what we would like to get. However, let us select a special gauge, which is frequently called (especially for the free space case, when $v = c$) the *Lorenz gauge condition*[70]

$$\nabla\cdot\mathbf{A} + \varepsilon\mu\frac{\partial\phi}{\partial t} = 0, \tag{6.117}$$

Lorenz gauge condition

[68] The situation with the *macroscopic* Maxwell equations is more complex, and is still a subject of some lingering discussions (usually called the *Abraham-Minkowski controversy*, despite contributions by many other scientists including A. Einstein), because of the ambiguity of the momentum's division between its field and particle components – see, e.g., the review paper by R. Pfeiffer *et al.*, *Rev. Mod. Phys.* **79**, 1197 (2007).

[69] We will return to their general discussion (in particular, to the analytical mechanics of the electromagnetic field, and its stress tensor) in Sec. 9.8, after we get equipped with the special relativity theory.

[70] This condition, named after *Ludwig Lorenz*, should not be confused with the so-called *Lorentz invariance condition* of relativity, due to *Hendrik Lorentz*, to be discussed in Sec. 9.4. (Note the last names' spelling.)

which is a natural generalization of the Coulomb gauge (5.48) to time-dependent phenomena. With this condition, Eqs. (107) are reduced to a simpler, beautifully symmetric form:

Potentials' dynamics

$$\nabla^2\phi - \frac{1}{v^2}\frac{\partial^2\phi}{\partial t^2} = -\frac{\rho}{\varepsilon}, \qquad \nabla^2\mathbf{A} - \frac{1}{v^2}\frac{\partial^2\mathbf{A}}{\partial t^2} = -\mu\mathbf{j}, \tag{6.118}$$

where $v^2 \equiv 1/\varepsilon\mu$. Note that these equations are essentially a set of 4 similar equations for 4 scalar functions (namely, ϕ and three Cartesian components of $\mathbf{A}$) and thus clearly invite the 4-component vector formalism of the relativity theory; it will be discussed in Chapter 9.[71]

If ϕ and $\mathbf{A}$ depend on just one spatial coordinate, say z, then in a region without field sources: $\rho = 0$, $\mathbf{j} = 0$, Eqs. (118) are reduced to the following 1D *wave equations*

$$\frac{\partial^2\phi}{\partial z^2} - \frac{1}{v^2}\frac{\partial^2\phi}{\partial t^2} = 0, \qquad \frac{\partial^2\mathbf{A}}{\partial z^2} - \frac{1}{v^2}\frac{\partial^2\mathbf{A}}{\partial t^2} = 0. \tag{6.119}$$

It is well known[72] that these equations describe waves, with arbitrary waveforms (including sinusoidal waves of any frequency), propagating with the same speed v in either of the z-axis directions. According to the definitions of the constants ε_0 and μ_0, in free space, v is just the speed of light:

$$v = \frac{1}{(\varepsilon_0\mu_0)^{1/2}} \equiv c\,. \tag{6.120}$$

Historically, the experimental observation of relatively low-frequency (GHz-scale) electromagnetic waves, with their speed equal to that of light, was the decisive proof (actually, a real triumph!) of the Maxwell theory and his prediction of such waves.[73] This was first accomplished in 1886 by Heinrich Rudolf Hertz, using the electronic circuits and antennas he had invented for this purpose.

Before proceeding to the detailed analysis of these waves in the following chapters, let me mention that the invariance of Eqs. (119) with respect to the wave propagation direction is not occasional; it is just a manifestation of one more general property of the Maxwell equations (99), called the *Lorentz reciprocity*. We have already met its simplest example, for time-independent electrostatic fields, in one of the problems of Chapter 1. In a much more general case when two monochromatic electromagnetic fields of the same frequency, with complex amplitudes, say, $\{\mathbf{E}_1(\mathbf{r}), \mathbf{H}_1(\mathbf{r})\}$ and $\{\mathbf{E}_2(\mathbf{r}),$

---

[71] Here I have to mention in passing the so-called *Hertz vector potentials* $\mathbf{\Pi}_e$ and $\mathbf{\Pi}_m$ (whose introduction may be traced back at least to the 1904 work by E. Whittaker). They may be defined by the following relations:

$$\mathbf{A} = \mu\frac{\partial\mathbf{\Pi}_e}{\partial t} + \mu\nabla\times\mathbf{\Pi}_m, \qquad \phi = -\frac{1}{\varepsilon}\nabla\cdot\mathbf{\Pi}_e,$$

which make the Lorentz gauge condition (117) automatically satisfied. These potentials are especially convenient for the solution of problems in which the electromagnetic field is induced by sources characterized by field-independent electric and magnetic polarizations $\mathbf{P}$ and $\mathbf{M}$ – rather than by field-independent charge and current densities ρ and $\mathbf{j}$. Indeed, it is straightforward to check that both $\mathbf{\Pi}_e$ and $\mathbf{\Pi}_m$ satisfy the equations similar to Eqs. (118), but with their right-hand sides equal to, respectively, $-\mathbf{P}$ and $-\mathbf{M}$. Unfortunately, I would not have time/space to discuss such problems and have to refer interested readers elsewhere – for example, to a classical text by J. Stratton, *Electromagnetic Theory*, Adams Press, 2008.

[72] See, e.g., CM Secs. 6.3-6.4 and 7.7-7.8.

[73] By that time, the speed of light (estimated very reasonably by Ole Rømer as early as 1676) has been experimentally measured, by Hippolyte Fizeau and then Léon Foucault, with an accuracy better than 1%.

$\mathbf{H}_2(\mathbf{r})\}$ are induced, separately, by stand-alone currents with complex amplitudes $\mathbf{j}_1(\mathbf{r})$ and $\mathbf{j}_2(\mathbf{r})$ of their densities. Then it may be proved[74] that if the medium is linear and either isotropic or even anisotropic but with symmetric tensors $\varepsilon_{jj'}$ and $\mu_{jj'}$, then for any volume V limited by a closed surface S,

$$\int_V \left(\mathbf{j}_1 \cdot \mathbf{E}_2 - \mathbf{j}_2 \cdot \mathbf{E}_1\right) d^3r = \oint_S \left(\mathbf{E}_1 \times \mathbf{H}_2 - \mathbf{E}_2 \times \mathbf{H}_1\right)_n d^2r \,. \tag{6.121}$$

This property implies, in particular, that the waves propagate similarly in two reciprocal directions even in situations much more general than the 1D case described by Eqs. (119). For some important practical applications (e.g., for low-noise amplifiers and detectors) such reciprocity is rather inconvenient. Fortunately, Eq. (121) may be violated in anisotropic media with asymmetric tensors $\varepsilon_{jj'}$ and/or $\mu_{jj'}$. The simplest case of such an anisotropy, the *Faraday rotation* of the wave polarization in plasma, will be discussed in the next chapter.

6.9. Exercise problems

6.1. Prove that the electromagnetic induction e.m.f. $\mathscr{V}_{\text{ind}}$ in a conducting loop may be measured as shown on two panels of Fig. 1:

(i) by measuring the current $I = \mathscr{V}_{\text{ind}}/R$ induced in the loop closed with an Ohmic resistor R, or

(ii) using a voltmeter inserted into the loop.

6.2. The flux Φ of the magnetic field that pierces a resistive ring is being changed in time, while the field outside of the ring is negligibly low. A voltmeter is connected to a part of the ring, as shown in the figure on the right. What would the voltmeter show?

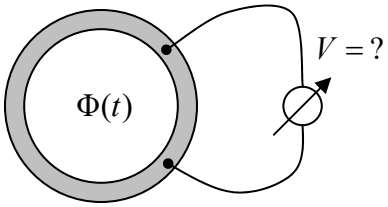

6.3. A weak constant magnetic field **B** is applied to an axially-symmetric permanent magnet with the dipole magnetic moment **m** directed along its axis, rapidly rotating about the same axis, with an angular momentum **L**. Calculate the electric field resulting from the magnetic field's application, and formulate the conditions of your result's validity.

6.4. The similarity of Eq. (5.53) obtained in Sec. 5.3 without any use of the Faraday induction law, and Eq. (5.54) proved in Sec. 2 of this chapter using it, implies that the law may be derived from magnetostatics. Prove that this is indeed true for a particular case of a current loop being slowly deformed in a fixed magnetic field **B**(**r**).

6.5. Could Problem 5.2 (i.e. the semi-quantitative analysis of the mechanical stability of the system shown in the figure on the right) be solved using potential energy arguments?

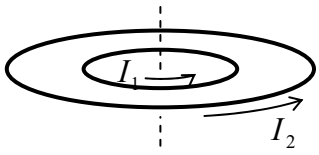

[74] It will be more convenient for me to give this proof (or rather offer it for the reader's exercise :-) in the next chapter, after we have discussed the Fourier expansion of the fields in linear media.

6.6. Use energy arguments to calculate the pressure exerted by the magnetic field **B** inside a long uniform solenoid of length l, and a cross-section of area $A << l^2$, with $N >> l/A^{1/2} >> 1$ turns, on its "walls" (windings), and the forces exerted by the field on the solenoid's ends, for two cases:

(i) the current through the solenoid is fixed by an external source, and

(ii) after the initial current setting, the ends of the solenoid's wire, with negligible resistance, are connected, so that it continues to carry a non-zero current.

Compare the results, and give a physical interpretation of the direction of these forces.

6.7. The *electromagnetic railgun* is a projectile launch system consisting of two long parallel conducting rails and a sliding conducting projectile shorting the current I fed into the system by a powerful source – see panel (a) in the figure on the right. Calculate the force exerted on the projectile, using two approaches:

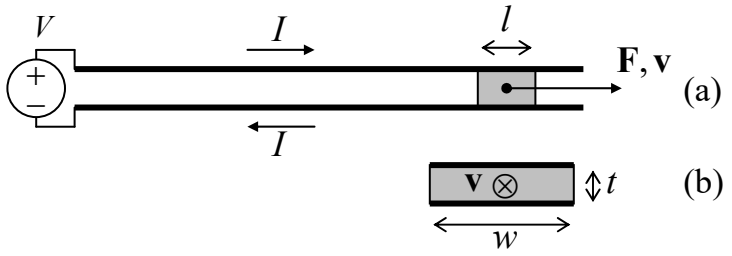

(i) by a direct calculation, assuming that the cross-section of the system has the simple shape shown on panel (b) of the figure above, with $t << w$, l, and

(ii) by using the energy balance (for simplicity, neglecting the Ohmic resistances in the system),

and compare the results.

6.8. A uniform, static magnetic field **B** is applied along the axis of a long thin pipe of a radius R and wall thickness $\tau << R$, made of a material with Ohmic conductivity σ. A sphere of mass M and radius $R' << R$, made of a linear magnetic material with permeability $\mu >> \mu_0$, is launched, with an initial velocity v_0, to fly ballistically along the pipe's axis – see the figure on the right. Use the quasistatic approximation to calculate the distance the sphere would pass before it stops. Formulate the conditions of validity of your result.

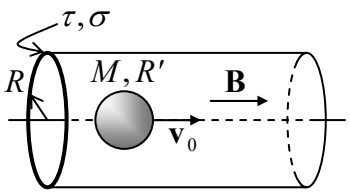

6.9. A planar thin-wire loop with inductance L, resistance R, and area A is launched to fly ballistically from field-free space into a region where the magnetic field **B** is constant. Calculate the final change of the kinetic energy of the loop, assuming that the time of its entry into the field region is much shorter than the relaxation time constant L/R and that the loop cannot rotate.

6.10. AC current of frequency ω is being passed through a long uniform wire with a round cross-section of a radius R comparable with the skin depth δ_s. In the quasistatic approximation, find the current's distribution across the cross-section, and analyze it in the limits $R << \delta_s$ and $\delta_s << R$. Calculate the effective ac resistance of the wire (per unit length) in these two limits.

6.11. A long round cylinder of radius R, made of a uniform conductor with an Ohmic conductivity σ and magnetic permeability μ, is placed into a uniform ac magnetic field $\mathbf{H}_{ext}(t) = \mathbf{H}_0 \cos\omega t$ directed along its symmetry axis. Calculate the spatial distribution of the magnetic field's amplitude and, in particular, its value on the cylinder's axis. Spell out the last result in the limits of relatively small and large R.

6.12.* Define and calculate an appropriate spatial-temporal Green's function for Eq. (25), and then use this function to analyze the dynamics of propagation of the external magnetic field that is suddenly turned on at $t = 0$ and then kept constant:

$$H(x<0,t)=\begin{cases}0, & \text{at } t<0,\\ H_0, & \text{at } t>0,\end{cases}$$

into an Ohmic conductor occupying the semi-space $x > 0$ – see Fig. 2.

Hint: Try to use a function proportional to $\exp\{-(x-x')^2/2(\delta x)^2\}$, with a suitable time dependence of the parameter δx and a properly selected pre-exponential factor.

6.13. Solve the previous problem using the variable separation method, and compare the results.

6.14. Calculate the average force exerted by ac current $I(t)$ of amplitude I_0, flowing in a planar round coil of radius R, on a conducting sphere with a much smaller radius R' (which is still much larger than the skin depth δ_s at the ac current's frequency), located on the loop's axis, at distance z from its center – see the figure on the right.

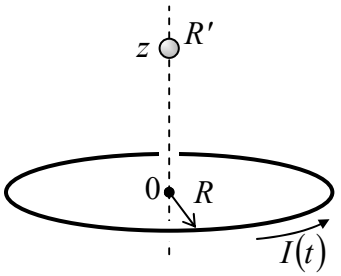

6.15. A small planar wire loop carrying current I is located relatively far from a planar surface of a superconductor. Within the coarse-grain (ideal-diamagnetic) description of the Meissner-Ochsenfeld effect, calculate:

(i) the energy of the loop-superconductor interaction,
(ii) the force and torque acting on the loop, and
(iii) the distribution of supercurrents on the superconductor surface.

6.16. A straight uniform magnet of length $2l$, cross-section area $A << l^2$, and mass m, with a permanent longitudinal magnetization M_0, is placed over a horizontal surface of a superconductor – see the figure on the right. Within the ideal-diamagnet description of superconductivity, find the stable equilibrium position of the magnet.

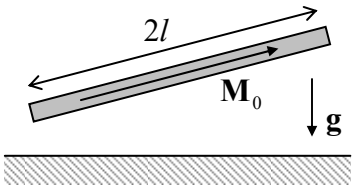

6.17. A plane superconducting wire loop of area A and inductance L may turn, without static friction, about a horizontal axis 0 (in the figure on the right, normal to the plane of the drawing) passing through its center of mass. Initially, the loop had been horizontal (with $\theta = 0$) and carried supercurrent I_0 in such a direction that its magnetic dipole vector had been directed down. Then a uniform magnetic field **B**, directed vertically up, was applied. Using the ideal-diamagnet description of the Meissner-Ochsenfeld effect, find all possible equilibrium positions of the loop, analyze their stability, and give a physical interpretation of the results.

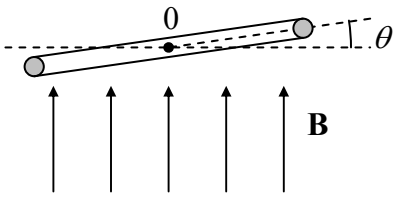

6.18. Use the London equation to analyze the penetration of a uniform external magnetic field into a thin ($t \sim \delta_L$) planar superconducting film whose plane is parallel to the field.

6.19. Use the London equation to calculate the distribution of supercurrent density **j** inside a long straight superconducting wire with a circular cross-section of radius $R \sim \delta_L$, carrying current I.

6.20. Use the London equation to calculate the inductance (per unit length) of a long uniform superconducting strip placed close to the surface of a similar superconductor – see the figure on the right, which shows the structure's cross-section.

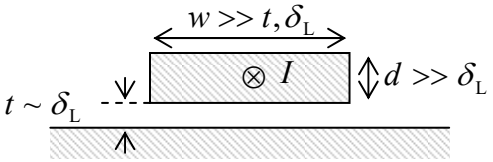

6.21. Calculate the inductance (per unit length) of a superconducting cable with the round cross-section shown in the figure on the right, in the following limits:

(i) $\delta_L << a, b, c - b$, and
(ii) $a << \delta_L << b, c - b$.

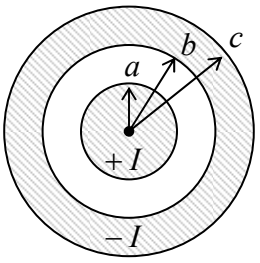

6.22. Use the London equation to analyze the magnetic field shielding by a superconducting thin film of thickness $t << \delta_L$, by calculating the penetration of the field induced by current I in a thin wire that runs parallel to a wide planar thin film, at a distance $d >> t$ from it, into the space behind the film.

6.23. Assuming that the magnetic monopole does exist and has a magnetic charge q_m, calculate the change ΔI of current in a superconducting loop due to a passage of a single monopole through its area. Evaluate ΔI for a monopole with the charge conjectured by P. Dirac, $q_m = nq_0 \equiv n(2\pi\hbar/e)$ with an integer n, and compare the result with the magnetic flux quantum Φ_0 (62). Review your result for a similar passage of a single quasi-monopole magnetic charge formed at one of the ends of a permanent-magnet needle – see, e.g., Fig. 19 and the accompanying discussion.

Hint: To simplify calculations, you may consider the monopole's passage along the symmetry axis of a round ring of radius R, made of a superconducting wire with a cross-section's area A satisfying the conditions $\delta_L^2 << A << R^2$.

6.24. Use the Ginzburg-Landau equations (54) and (63) to calculate the largest ("critical") value of supercurrent in a uniform superconducting wire with a cross-section area much smaller than δ_L^2.

6.25. Use the discussion of a long straight Abrikosov vortex, in the limit $\xi << \delta_L$, in Sec. 5 to prove Eqs. (71)-(72) for its energy per unit length and the first critical field.

6.26.* Use the Ginzburg-Landau equations (54) and (63) to prove the Josephson relation (76) for a small superconducting weak link, and express its critical current I_c via the Ohmic resistance R_n of the same weak link in its normal state.

6.27. Use Eqs. (76) and (79) to calculate the coupling energy of a Josephson junction and the full potential energy of the SQUID shown in Fig. 4c.

6.28. Analyze the possibility of wave propagation in a long uniform chain of lumped inductances and capacitances – see the figure on the right.

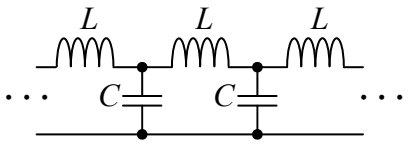

Hint: Readers without prior experience in electromagnetic wave analysis may like to use a substantial analogy between this effect and mechanical waves in a 1D chain of elastically coupled particles.[75]

6.29. A sinusoidal e.m.f. of amplitude V_0 and frequency ω is applied to an end of a long chain of similar lumped resistors and capacitors, shown in the figure on the right. Calculate the law of decay of the ac voltage amplitude along the chain.

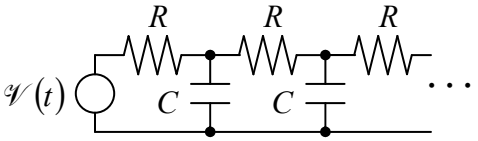

6.30. As was discussed in Sec. 7, the displacement current concept allows one to extend the Ampère law to time-dependent processes as

$$\oint_C \mathbf{H}\cdot d\mathbf{r} = I_S + \frac{\partial}{\partial t}\int_S D_n d^2 r\,.$$

We also have seen that this generalization makes the integral $\int \mathbf{H}\cdot d\mathbf{r}$ over an external contour, such as the one shown in Fig. 10, independent of the choice of the surface S limited by the contour. However, it may look like the situation is different for a contour drawn inside a capacitor – see the figure on the right. Indeed, if the contour's size is much larger than the capacitor's thickness, the magnetic field $\mathbf{H}$ created by the linear current I on the contour's line is virtually the same as that of a continuous wire, and hence the integral $\int \mathbf{H}\cdot d\mathbf{r}$ along the contour apparently does not depend on its area, while the magnetic flux $\int D_n d^2 r$ does, so the equation displayed above seems invalid. (The current I_S piercing this contour evidently equals zero.) Resolve this paradox, for simplicity considering an axially-symmetric system.

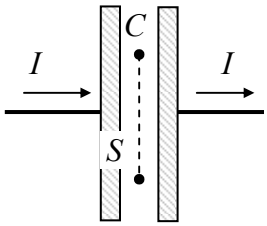

6.31. A straight, uniform, long wire with a circular cross-section of radius R, made of an Ohmic conductor with conductivity σ, carries dc current I. Calculate the flux of the Poynting vector through its surface, and compare it with the Joule rate of energy dissipation.

[75] See, e.g., CM Sec. 6.3.